文　献

1) Takahashi N, et al: Osteoblastic cells are involved in osteoclast formation. Endocrinology 123: 2600–2602, 1988.
2) Yasuda H, et al: Osteoclast differentiation factor is a ligand for osteoprotegerin/osteoclastogenesis inhibitory factor and is identical to TRANCE/RANKL. Proc Natl Acad Sci USA 95: 3597–3602, 1998.
3) Wong B R, et al: TRANCE is a novel ligand of the tumor necrosis factor receptor family that activates c-Jun N-terminal kinase in T cells. J Biol Chem 272: 25190–25194, 1997.
4) Anderson D M, et al: A homologue of the TNF receptor and its ligand enhance T-cell growth and dendritic-cell function. Nature 390: 175–179, 1997.
5) Suda T, et al: Modulation of osteoclast differentiation and function by the new members of the tumor necrosis factor receptor and ligand families. Endocr Rev 20: 345–357, 1999.
6) Takami M, et al: Intracellular calcium and protein kinase C mediate expression of receptor activator of nuclear factor κB ligand and osteoprotegerin in osteoblasts. Endocrinology 141: 4711–4719, 2000.
7) Akira S, et al: Toll-like receptors: critical proteins linking innate and acquired immunity. Nat Immnol 2: 675–680, 2001.
8) Alexopoulou L, et al: Hyporesponsiveness to vaccination with *Borrelia burgdorferi* OspA in humans and in TLR1- and TLR2-deficient mice. Nat Med 8: 878–884, 2002.
9) 須田幸治, 他: LPS はプロスタグランジン E_2 を介さず RANKL の発現を上昇させ破骨細胞形成を誘導する. 日本骨代謝学会プログラム抄録号, p102, 2002.
10) Kikuchi T, et al: Gene expression of osteoclast differentiation factor is induced by lipopolysaccharide in mouse osteoblasts via toll-like receptor. J Immunol 166: 3574–3579, 2001.
11) Dumitru C D, et al: TNFα induction by LPS is regulated posttranscriptionally via a Tpl2/ERK-dependent pathway. Cell 103: 1071–1083, 2000.
12) Kikuchi T, et al: Cot/Tpl2 is essential for RANKL induction by lipid A in osteoblasts. J Dent Res 82: 546–550, 2003.
13) 佐藤信明, 他: Toll 様受容体リガンド誘導性破骨細胞分化は MyD88 が必須である. 日本骨代謝学会プログラム抄録号, p40, 2003.
14) Takami M, et al: Stimulation of Toll-like receptors inhibits osteoclast differentiation. J Immunol 169: 1516–1523, 2002.
15) Li X, et al: p38 MAPK-mediated signals are required for inducing osteoclast differentiation but not for osteoclast function. Endocrinology 143: 3105–3113, 2002.
16) Suda K, et al: Lipopolysaccharide supports survival and fusion of preosteoclasts independent of TNFα, IL-1, and RANKL. J Cell Physiol 190: 101–108, 2002.
17) Itoh K, et al: Lipopolysaccharide promotes the survival of osteoclasts via Toll-like receptor 4, but cytokine production of osteoclasts in response to lipopolysaccharide is different from that of macrophages. J Immunol 170: 3688–3695, 2003.
18) Wong B R, et al: TRANCE, a TNF family member, activates Akt/PKB through a signaling complex involving TRAF6 and c-Src. Mol Cell 4: 1041–1049, 1999.
19) Takayanagi H, et al: Induction and activation of the transcription factor NFATc1 (NFAT2) integrate RANKL signaling terminal differentiation of osteoclasts. Dev Cell 3: 889–901, 2002.
20) Ishida N, et al: Large scale gene expression analysis of osteoclastogenesis *in vitro* and elucidation of NFAT2 as a key regulator. J Biol Chem 277: 41147–41156, 2002.
21) Horsley V, et al: Regulation of the growth of multinucleated muscle cells by NFATC2-dependent pathway. J Cell Biol 153: 329–338, 2001.
22) Lacey D L, et al: Osteoprotegerin ligand is a cytokine that regulates osteoclast differentiation and activation. Cell 93: 165–176, 1998.
23) Takayanagi H, et al: T-cell-mediated regulation of osteoclastogenesis by signalling cross-talk between RANKL and IFN-γ. Nature 408: 600–605, 2000.
24) Takayanagi H, et al: RANKL maintains bone

homeostasis through c-Fos-dependent induction of interferon-β. Nature 416: 744-749, 2002.

Regulatory Mechanisms of Bone Resorption

Yasuhiro Kobayashi[1], Nobuyuki Udagawa[2], Naoyuki Takahashi[1]
[1] Division of Hard Tissue Research, Institute for Oral Science, Matsumoto Dental University
[2] Department of Biochemistry, Matsumoto Dental University

MOLECULAR AND CELLULAR BIOLOGY, Jan. 2003, p. 636–644 Vol. 23, No. 2
0270-7306/03/$08.00+0 DOI: 10.1128/MCB.23.2.636–644.2003

Chondromodulin I Is a Bone Remodeling Factor

Yuko Nakamichi,[1,2] Chisa Shukunami,[3] Takashi Yamada,[1,4] Ken-ichi Aihara,[1] Hirotaka Kawano,[4] Takashi Sato,[1,5] Yuriko Nishizaki,[3] Yoko Yamamoto,[1] Masayo Shindo,[1] Kimihiro Yoshimura,[1] Takashi Nakamura,[1] Naoyuki Takahashi,[2] Hiroshi Kawaguchi,[4] Yuji Hiraki,[3] and Shigeaki Kato[1,5]*

The Institute of Molecular and Cellular Biosciences,[1] and The Department of Orthopedic Surgery, Faculty of Medicine,[4] University of Tokyo, Bunkyo-ku, Tokyo, The Institute for Oral Science, Matsumoto Dental University, Hiro-oka, Shiojiri, Nagano[2], The Institute for Frontier Medical Sciences, Kyoto University, Sakyo-ku, Kyoto,[3] and CREST, Japan Science and Technology, Kawaguchi, Saitama,[5] Japan

Received 10 May 2002/Returned for modification 11 July 2002/Accepted 21 October 2002

Chondromodulin I (ChM-I) was supposed from its limited expression in cartilage and its functions in cultured chondrocytes as a major regulator in cartilage development. Here, we generated mice deficient in ChM-I by targeted disruption of the *ChM-I* gene. No overt abnormality was detected in endochondral bone formation during embryogenesis and cartilage development during growth stages of ChM-I$^{-/-}$ mice. However, a significant increase in bone mineral density with lowered bone resorption with respect to formation was unexpectedly found in adult ChM-I$^{-/-}$ mice. Thus, the present study established that ChM-I is a bone remodeling factor.

Endochondral bone development during embryogenesis and longitudinal bone growth in growing vertebrates require continuous cartilage growth (18). Proliferating chondrocytes originate from a region of resting chondrocytes, differentiate first into prehypertrophic chondrocytes and then into hypertrophic chondrocytes able to secrete the cartilage matrix. Through invasion by blood vessels, the calcified cartilage and vascular matrix are gradually replaced by bone matrix with the recruitment of osteoclasts and osteoblasts that mediate bone resorption and formation and eventual bone remodeling (1, 30). Thus, in bone growth, blood vessel invasion into cartilage is pivotal to the process of endochondral bone formation.

Distinct classes of factors are thought to play cognate roles in the spatiotemporal regulation of the complicated yet sequential processes of cartilage differentiation and bone formation, particularly in angiogenic events. Fibroblast growth factor-2 (5, 31), transforming growth factor β (3), and vascular endothelial growth factor (4) are expressed in cartilage and have been identified as strong angiogenic agents. However, these factors are also present in avascular cartilage and in surrounding vascular regions. These findings raise the possibility that the actions of angiogenic factors may be suppressed by the inhibitory action of a specific factor in avascular cartilage. While tissue inhibitors of matrix metalloproteinase 1 and 2 have been identified from cartilage as possible angiogenesis inhibitors, they are also expressed in other tissues (20). The search for a cartilage-specific inhibitor of angiogenesis led to the identification of chondromodulin I (ChM-I), initially isolated from bovine epiphyseal cartilage as a factor with growth-promoting activity on cultured chondrocytes (10). ChM-I was found to be a potent stimulator of proteoglycan synthesis in growth plate chondrocytes and of chondrocyte colony formation in agarose (12). However, ChM-I inhibited cultured vascular endothelial cell tube morphogenesis and growth (8, 9). Thus, the physiological significance of ChM-I during endochondral bone formation as a bifunctional factor of chondrocyte growth and angiogenesis inhibition was suggested from distinct lines of evidence in vitro (27). However, due to the lack of mice deficient in ChM-I, there has been no information regarding the physiological role of ChM-I.

In the present study, we disrupted the murine *ChM-I* gene by homologous recombination to generate *ChM-I* knockout (*ChM-I*$^{-/-}$) mice. Homozygous *ChM-I*$^{-/-}$ mice were born without overt abnormalities and grew normally. Unexpectedly, *ChM-I*$^{-/-}$ mice exhibited no aberrations in endochondral bone formation during embryogenesis or in cartilage development during growth stages. However, a significant increase in bone mineral density was observed in 12-week-old *ChM-I*$^{-/-}$ mice. Analyses of bone formation and resorption indicators revealed that bone minerals accumulated in *ChM-I*$^{-/-}$ mice due to lowered bone resorption with respect to formation. Thus, our study revealed that the physiological role of ChM-I appears to be involved in the stimulation of bone remodeling through control of osteoclast and osteoblast functions rather than in cartilage development in intact animals.

MATERIALS AND METHODS

Gene targeting. A TT2 embryonic stem (ES) cell (34) genomic library was screened with a mouse ChM-I cDNA probe (24). A 9-kb fragment of mouse ChM-I containing the coding exons 1 to 3 was used to construct a targeting vector. A stop mutation was introduced at the beginning of the ChM-I coding region, and 3.5-kb fragment containing exon 3 was replaced with a phosphoglycerate kinase-neomycin cassette. TT2 ES cells were transfected with a linearized targeting vector (25 μg per 1.0×10^7 cells) by using a Bio-Rad Gene Pulser II at 250 V and 500 μF and grown under G418 selection as described previously (23, 36). Targeted ES cell clones were identified by Southern blot analysis with probe A and probe NEO (Fig. 1A) and were aggregated with CD-1 single 8-cell embryos to generate chimeras as described previously (23, 36). Chimeras were crossed with C57BL/6 female mice to produce germ line transmission of the targeted allele. Offspring were genotyped either by Southern blotting with probe A or by PCR with the three specific primers P1 (5′-TTGGTTGATGCTTCAG

* Corresponding author. Mailing address: The Institute of Molecular and Cellular Biosciences, University of Tokyo, 1-1-1 Yayoi, Bunkyo-ku, Tokyo 113-0032, Japan. Phone: 81-3-5841-8478. Fax: 81-3-5841-8477. E-mail: uskato@mail.ecc.u-tokyo.ac.jp.

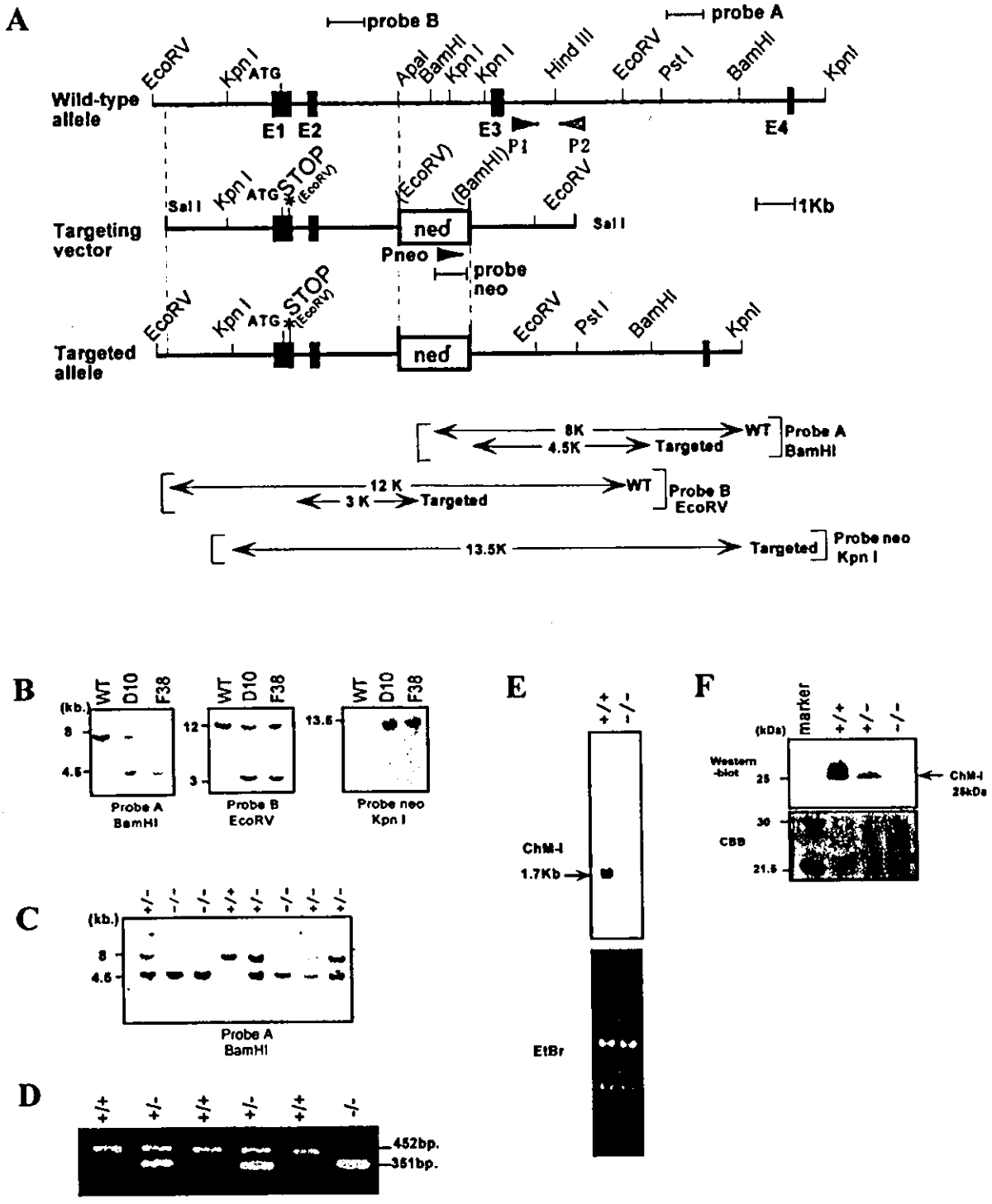

FIG. 1. Disruption of the mouse ChM-I gene. (A) Schematic representation of the *ChM-1* gene locus (top), gene targeting vector (middle), and the recombinated locus (bottom).The digested fragments detected by probe A, probe B, and probe NEO are indicated by bars. (B) Southern blot analysis of targeted ES clones. The targeting frequency was 0.3%. The presence of the 4.5-kb *Bam*HI fragment indicates proper targeting of the ChM-I locus, and the 3-kb *Eco*RV fragment indicates the introduction of the stop mutation. (C) Southern blot analysis of tail DNA from the offspring of heterozygous mates with probe A as described for panel B. (D) PCR genotyping of embryos at e13.5 of heterozygous matings with three primers (P1, P2, Pneo) as indicated in panel A. Primer 1 and primer 2 were used to detect the wild-type (WT) allele (amplification of a 452-bp fragment). Primer 2 and primer NEO were used to detect the targeted allele (amplification of a 351-bp fragment). (E) Northern blot analysis of RNA from *ChM-1*$^{+/+}$ and *ChM-1*$^{-/-}$ mice in the top panel. The bottom panel shows ethidium bromide (EtBr) staining of the RNA used. (F) Western blot analysis confirming the absence of ChM-I protein with an anti-rhChM-I polyclonal antibody. The top panel shows the immunoreactivity after hybridization with anti-ChM-I antibody. The bottom panel shows Coomassie brilliant blue staining of the SDS-polyacrylamide gel electrophoresis gel.

TGTG-3'), P2 (5'-CTTGTGCACAGACCAGAACAA-3'), and Pneo (5'-CCG CTTCCTCGTGCTTTACGG-3'). Temperature cycling conditions were as follows: denaturation at 95°C for 2 min followed by 35 cycles of 95°C for 1 min, 54°C for 1 min, and 72°C for 1.5 min.

Northern blot analysis. Total RNA was prepared from rib cartilage of 3- to 4-week-old *ChM-I*$^{+/+}$ or *ChM-I*$^{-/-}$ mice by a single-step method (35). Total RNA (15 μg) was separated by electrophoresis on a 1% agarose formaldehyde gel and transferred onto a Nytran filter with Turboblotter (Schleicher and Schuell). The filter was then hybridized with a ^{32}P-labeled probe that is an 822-bp *Eco*RI fragment from nucleotides 628 to 1449 of the ChM-I cDNA. After hybridization, the filter was washed at 55°C for 30 min in 1× SSPE (1× SSPE is 0.18 M NaCl, 10 mM NaH_2PO_4, and 1 mM EDTA [pH7.7])–0.1% sodium dodecyl sulfate (SDS) once, then washed at 55°C for 30 min in 0.1× SSPE–0.1% SDS twice. The filter was exposed to BIOMAX film (Eastman Kodak) at −80°C.

Western blot analysis. Whole ribs from 3-week-old mice were homogenized in extraction buffer {20 mM MES [2-(*N*-morpholino)ethanesulfonic acid]-NaOH [pH 6.0], 0.1 M aminocaproate, 6 M guanidium chloride} at 4°C and centrifuged at 10,000 × *g*. The supernatant was diluted with 2 volumes of distilled water and applied to a butyl-toyopearl 650 affinity column OSOH. The column was washed three times with distilled water. Bound proteins were eluted by 70% ethanol and dried. The dried materials (8 μg) were dissolved in Laemmli buffer, electrophoresed by SDS–15% polyacrylamide gel electrophoresis, and blotted onto an Immobilon-P membrane (Millipore). Bands that were immunoreactive with an anti-ChM-I polyclonal antibody for the C-terminal peptides of the mature form of human ChM-I, corresponding to the Asp^{252} to Val^{334} residues, which is a highly conserved region among species (26), were stained by using enhanced chemiluminescence methods (Amersham Biosciences).

Morphology and histological analyses. For cleared skeletal preparations (23), embryos from embryonic day 13.5 (e13.5) were fixed in 99.5% ethanol for 4 days and transferred to acetone. After 3 days, they were rinsed with water and stained for 10 days in a staining solution consisting of 1 volume of 0.1% Alizarin red S (Sigma) in 95% ethanol, 1 volume of 0.3% Alcian blue 8GX (Sigma) in 70% ethanol, 1 volume of 100% acetic acid, and 17 volumes of ethanol. After rinsing with 96% ethanol, specimens were kept in 20% glycerol–1% KOH at room temperature until the skeletons became clearly visible. For hematoxylin-fast green-safranin O staining, bones were fixed in 4% paraformaldehyde overnight and decalcified in Morse's solution (10% [wt/vol] sodium citrate, 22.5% [vol/vol] formic acid) overnight prior to embedding in paraffin. For Villanueva Goldner, toluidine blue, and tartartic acid resistance alkaline phosphatase (TRAP) staining, tibiae were embedded in glycolmethacrylate without decalcification (36) (see below).

Bone radiographic analysis and histomorphometry. For radiographic analysis, femora from male weight-matched mice were dissected free of soft tissues and subjected to radiographic analysis with a soft X-ray apparatus (model CMB-2; SOFTEX) (36). Bone mineral density was measured by dual energy X-ray absorptiometry with a bone mineral analyzer (PIXImus2; GE Medical Systems). For in vivo fluorescent labeling (21), a single intraperitoneal injection of calcein (1.6 mg/kg of body weight) was administrated at days 0 and 4. Mice were sacrificed at day 5. Tibiae were fixed in 99.5% ethanol and embedded in glycolmethacrylate without decalcification. Longitudinal serial sections (7 μm thick) were prepared with a microtome (model 2050; Reichert Jung). The sections were stained with Villanueva Goldner to discriminate between mineralized and unmineralized bone and to identify cellular components (36). Images were visualized by fluorescent microscopy. Histomorphometry of bone sections was performed for at least eight optical fields of the secondary spongiosa with a semiautomated system for bone analysis (Osteoplan II; Carl Zeiss) at 200-fold magnification (17). All sections were examined blind. Nomenclature, symbols, and units are those recommended by the Nomenclature Committee of the American Society for Bone and Mineral Research (22).

Reverse transcription-PCR analysis. For the isolation osteoblasts for primary culture, calvaria from newborn C57BL/6 mice were dissected into pieces with scissors and cultured in α-minimal essential medium (α-MEM) containing 10% heat-inactivated fetal bovine serum (FBS) at 37°C in 5% CO_2. After the cells were grown to subconfluence, total cellular RNA was extracted as previously described (35). Femora and tibiae were dissected free of adherent tissues and epiphyseal cartilage, and the bone marrow was flushed out. The total RNA of the bone was prepared from several mice (12-week-old mice). For isolation of osteoclasts, primary calvarial osteoblasts (1.5×10^4 cells/dish) and bone marrow cells (10^5 cells/dish) were cocultured in α-MEM supplemented with 10% FBS, 1α,25-dihydroxy vitamin D_3 (10^{-8} M) and prostaglandin E_2 (10^{-6} M) in 100-mm-diameter dishes precoated with type I collagen gel (cell matrix type-IA; Nitta Gelatin) (28). Osteoclasts were formed within 7 days in the coculture, and differentiated osteoclasts were collected as described previously (16). The purified osteoclasts in this preparation were subjected to total RNA extraction. First-strand cDNA was synthesized from total RNA with oligo$(dT)_{12-18}$ primer with the Super Script II preamplification system (Life Technologies) and subjected to PCR amplification with Ex *Taq* polymerase (TaKaRa) and the specific pair of primers mChM-If (in exon 5) (5'-CTTAAGCCCATGTATCCAAA-3') and mChM-Ir (in exon 7) (5'-CCAGTGGTTCACAGATCTTC-3'). Temperature cycling conditions were as follows: denaturation at 96°C for 3 min followed by 30 cycles of 96°C for 30s, 60°C for 1 min, and 72°C for 30s.

In vitro osteoclastogenesis. Bone marrow macrophages were isolated from whole tibial bone marrow of 12-week-old mice ($n = 3$) and cultured in α-MEM containing 10% heat-inactivated FBS at 37°C in 5% CO_2 (16). After 24 h in culture, the nonadherent cells were collected and replaced in a 96-well plate (2×10^5 cells/well) in α-MEM supplemented with 10% heat-inactivated FBS at 37°C in 5% CO_2 in the presence of 100 ng of recombinant human macrophage colony-stimulating factor (rhM-CSF) (leukoprol; Kyowa Hakko Kogyo)/ml. Cells were stimulated with 100 ng of soluble recombinant human receptor activator of nuclear factor-κB ligand (rhRANKL; Pepro Teck EC Ltd.)/ml on day 4 in the presence of 100 ng of rhM-CSF/ml. Cells were fixed and stained for TRAP as described previously (29) on day 9 or 10. TRAP-positive multinucleated cells containing three or more nuclei were counted as osteoclasts under microscopic examination. The results were expressed as the means ± standard deviations of four wells.

Serum and urinary indicators. Blood from 12-week-old male mice was collected by heart puncture under nembutal (Dainippon Pharmaceutical Co.) anesthesia. The levels of calcium, phosphorus, and alkaline phosphatase activity in serum were measured by using a calcium HR kit (Wako), inorganic phosphorus II kit (Wako), and liquitech alkaline phosphatase kit (Roche Diagnostic), respectively, with an autoanalyzer (type 7170; Hitachi) (36). The levels of osteocalcin in serum were measured by using the competitive radioimmunoassay kit by Biomedical Technologies, Inc. The urinary excretion of deoxypyridinoline cross-links, a marker of bone resorption (32), was measured in urine samples by using the Pyriliks-D enzyme-linked immunosorbent assay (Metra Biosystems). Results were expressed in nanomoles per millimole of urinary creatinine (Cr), as measured by a standard colorimetric technique with an autoanalyzer (type 7170; Hitachi).

RESULTS

Generation of targeted ChM-I-null mice. We disrupted the murine *ChM-I* gene in ES cells by homologous recombination to generate *ChM-I*$^{-/-}$ mice. The targeting vector (Fig. 1A) was constructed to introduce a stop codon at Cys-21, and a 3.5-kb genomic fragment containing exon 3 was replaced by a phosphoglycerate kinase-neomycin cassette. No overt abnormalities were found in *ChM-I*$^{+/-}$ mice, and crossbreeding of *ChM-I*$^{+/-}$ mice produced normal numbers of pups of all three possible genotypes (Fig. 1C) with the expected Mendelian distribution (61 +/+ mice, 128 +/− mice, and 56 −/− mice, for a total of 245 offspring) (Fig. 1B and C). Northern blot analysis of rib cartilage from normal mice with a cDNA probe encoding the mature form of ChM-I protein detected a single 1.7-kb transcript. No transcripts were found in *ChM-I*$^{-/-}$ mice, confirming the disruption of the *ChM-I* gene (Fig. 1E). Western blot analysis of whole-rib extracts from *ChM-I*$^{-/-}$ mice with an antibody against the mature ChM-I protein also confirmed the absence of the ChM-I protein (Fig. 1F).

ChM-I is not required for cartilage development and endochondral bone formation. *ChM-I*$^{-/-}$ mice grew normally with no discernible physical defects and with normal fertility. As ChM-I had been implicated in cartilage development, endochondral bone formation, and morphogenesis of the eye, careful histological examination of these tissues from *ChM-I*$^{-/-}$ mouse embryos and mice at various growth stages was performed. However, we failed to defect any abnormalities in cartilage formation (Fig. 2A), first ossification (Fig. 2B) in *ChM-I*$^{-/-}$ fetuses, and secondary ossification in *ChM-I*$^{-/-}$

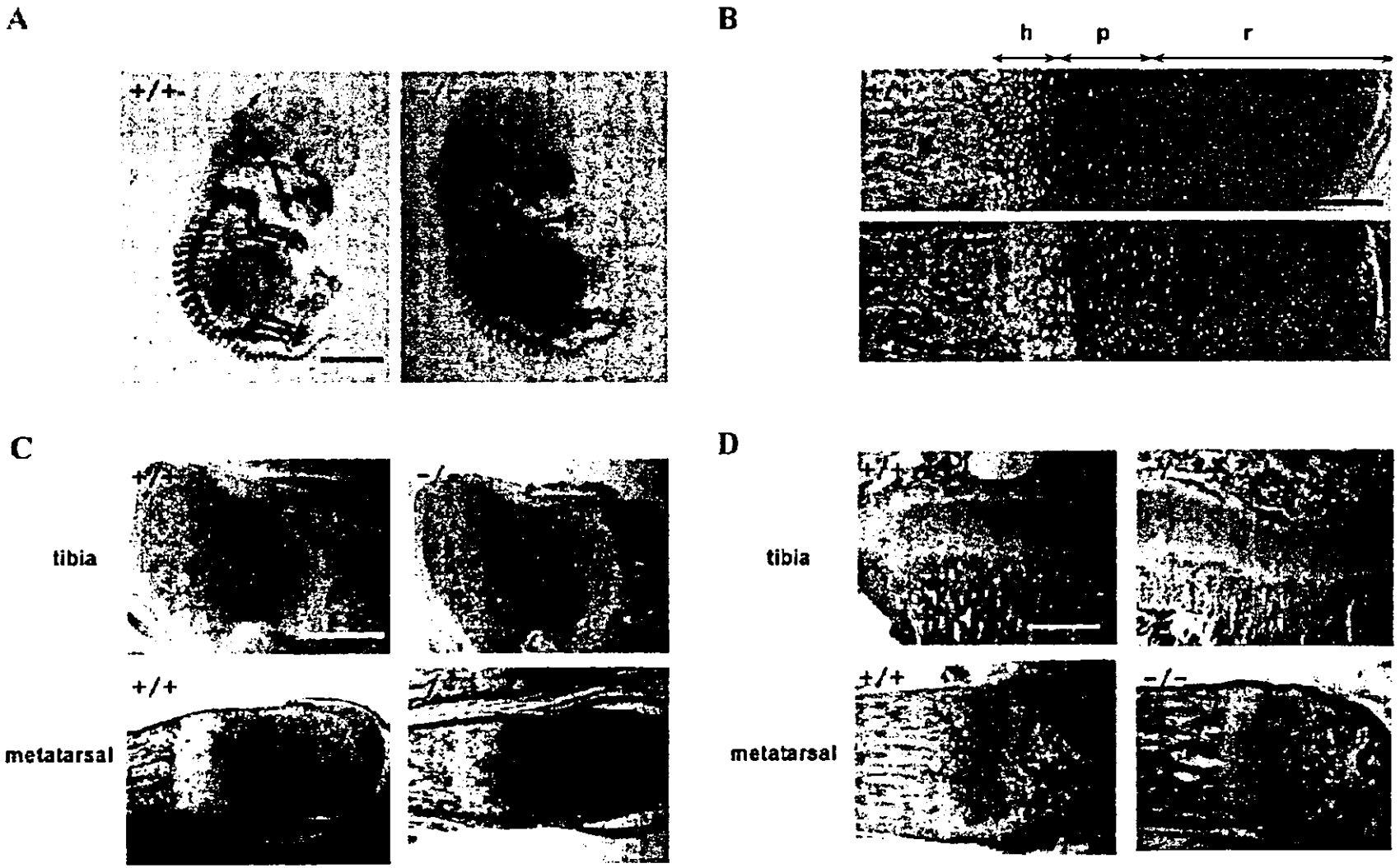

FIG. 2. No abnormality in cartilage development and endochondral bone formation of *ChM-I*$^{-/-}$ mice. (A) Alizarin red and Alcian blue staining of e13.5 embryos. Bar, 2 mm. (B) Safranin O-fast green-hematoxylin staining of proximal growth plate of tibiae from e18.5 embryos. Bar, 0.1 mm. h, hypertrophic zone; p, proliferating zone; r, resting zone. (C) Safranin O-fast green-hematoxylin staining of epiphyses from 1-week-old mice. Bar, 0.5 mm. (D) Safranin O-fast green-hematoxylin staining of epiphyses from 3-week-old mice. Bar, 0.5 mm. In all panels, no overt difference was detected between *ChM-I*$^{+/+}$ and *ChM-I*$^{-/-}$ mice.

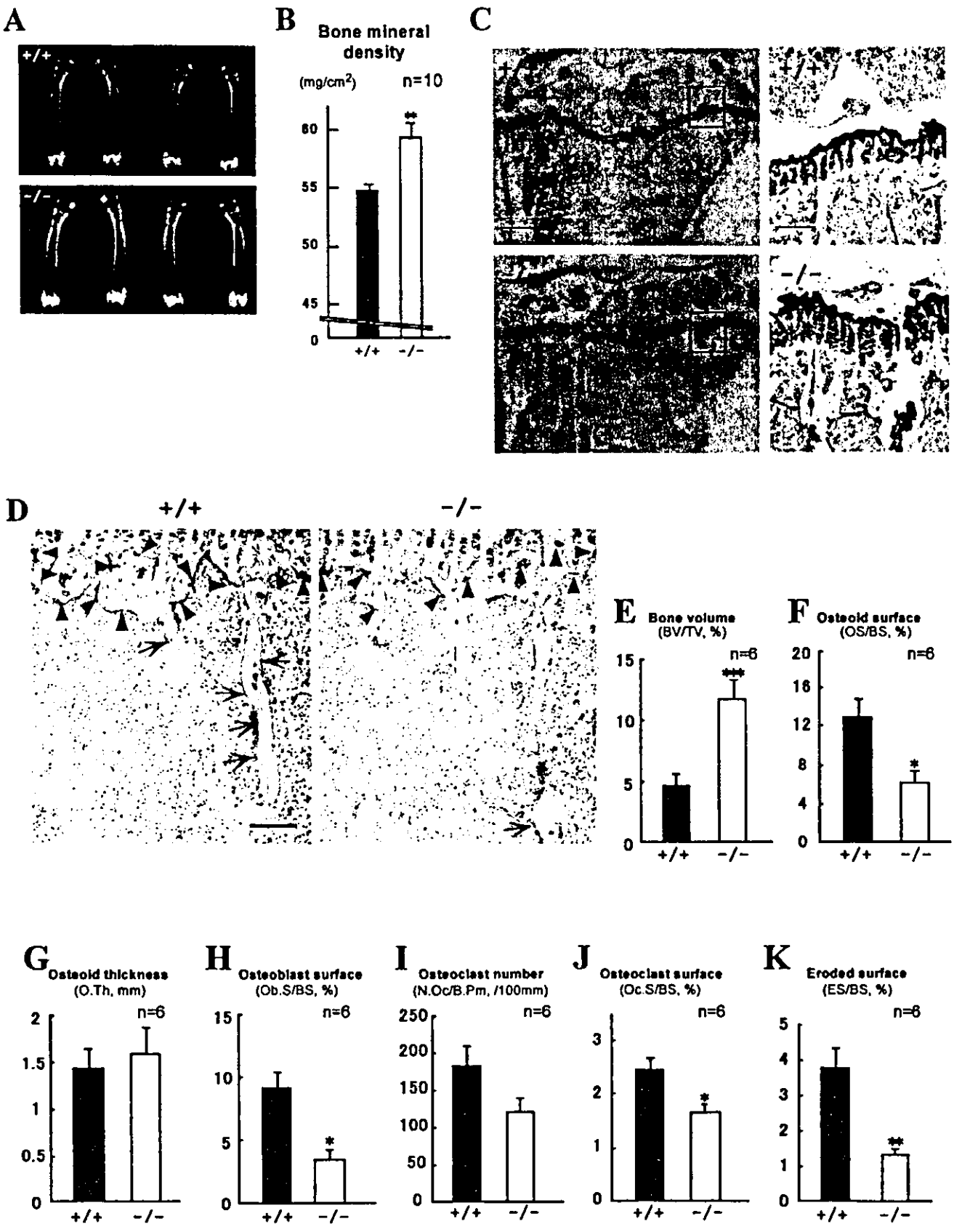
A
+/+
-/-
B
Bone mineral density
(mg/cm²)
n=10
**
60
55
50
45
0
+/+
-/-
C
+/+
-/-
D
+/+
-/-
E
Bone volume
(BV/TV, %)
n=6
***
15
10
5
0
+/+
-/-
F
Osteoid surface
(OS/BS, %)
n=6
20
16
12
8
4
0
*
+/+
-/-
G
Osteoid thickness
(O.Th, mm)
n=6
2
1.5
1
0.5
0
+/+
-/-
H
Osteoblast surface
(Ob.S/BS, %)
n=6
15
10
5
0
*
+/+
-/-
I
Osteoclast number
(N.Oc/B.Pm, /100mm)
n=6
250
200
150
100
50
0
+/+
-/-
J
Osteoclast surface
(Oc.S/BS, %)
n=6
3
2
1
0
*
+/+
-/-
K
Eroded surface
(ES/BS, %)
n=6
5
4
3
2
1
0
**
+/+
-/-

mice at 1 and 3 weeks old (Fig. 2C and D), in agreement with normal growth of *ChM-I*$^{-/-}$ mice.

Mice homozygous for the ChM-I mutation exhibit increased bone mineral density. Unexpectedly, a significant increase in bone mineral density was observed in 12-week-old *ChM-I*$^{-/-}$ mice but not in *ChM-I*$^{+/-}$ mice. Also, the radiographic mineral density of the femur in mutant mice was approximately 10% higher than in wild-type mice (Fig. 3A and B). Histomorphometric analyses confirmed that trabecular bone volumes (bone volume per tissue volume) in mutant mice were 2.5-fold higher than in wild-type mice (Fig. 3C and E). However, no significant differences in bone or body size and shape were observed between *ChM-I*$^{-/-}$ and wild-type mice. Osteoid surfaces (osteoid surface per bone surface) in mutant mice were 54% lower than in wild-type mice (Fig. 3F), but the osteoid thickness value in mutant mice was equivalent to that in wild-type mice (Fig. 3G). Indeed, the expression of the ChM-I gene was detected in the primary culture osteoblasts and total bone, though their expression levels appear to be much lower than those in cartilage (Fig. 4).

As it was possible that the observed increase in bone mineral density was related to bone remodeling (2), we studied bone formation and resorption in terms of osteoblast and osteoclast function. TRAP-positive mature osteoclast and chondroclast numbers were reduced in *ChM-I*$^{-/-}$ mice (Fig. 3D). This was in agreement with the results of histomorphometry analyses that showed that the numbers of bone osteoclasts (osteoclast number per bone perimeter) and surface osteoclasts (osteoclast surface per bone surface) in *ChM-I*$^{-/-}$ mice were 33 and 34% lower than in wild-type mice, respectively (Fig. 3H and I). Eroded surface (eroded surface per bone surface) values, which represent osteoclast activity, were also significantly decreased in *ChM-I*$^{-/-}$ mice (Fig. 3J). In addition, osteoblast surface (osteoblast surface per bone surface) values, a reliable histomorphometric indicator of active osteoblast numbers, were significantly reduced to approximately 60% by *ChM-I* inactivation (Fig. 3K). Reflecting the reduced osteoclast and/or chondroclast activity in *ChM-I*$^{-/-}$ mice, more cartilaginous matrix remained in the first spongiosa of tibiae in the *ChM-I*$^{-/-}$ mice than in wild-type mice (Fig. 3C, right).

Loss of ChM-I affects bone metabolism. We then estimated the bone formation rate directly by using calcein double-labeling of the mineralized matrix (22). Both the mineral apposition rate (MAR) and bone formation rate (BFR) (BFR per bone surface) were significantly decreased in *ChM-I*$^{-/-}$ mice (Fig. 5A, B, and C). Reduced levels in serum of markers for osteoblastic function (alkaline phosphatase activity and osteocalcin) (Fig. 5E and F) and no alteration in serum minerals (Fig. 5G, H) supported the hypothesis that bone formation activity was reduced by *ChM-I* inactivation. Total urinary deoxypyridinoline levels, a marker of bone resorption, were measured by enzyme-linked immunosorbent assay; however, no statistical difference was observed between wild-type and *ChM-I*$^{-/-}$ mice (Fig. 5D). Moreover, in vitro osteoclastogenesis with donor bone marrow macrophages from mutant and wild-type mice revealed that *ChM-I* inactivation appears to cause no abnormality in osteoclastogenesis (Fig. 6). Our results indicated that the increased bone mineral density in *ChM-I*$^{-/-}$ mice appeared to be due to lowered bone resorption with respect to bone formation. Thus, the present study established that ChM-I is likely to be a bone remodeling factor rather than being involved in chondrocyte development.

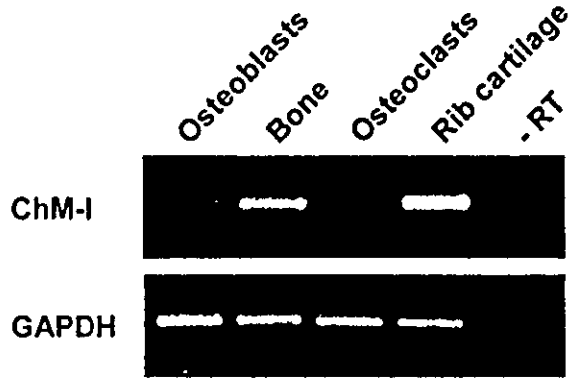

FIG. 4. ChM-I mRNA expression in bone. The top panel shows the ChM-I transcripts. The bottom panel shows glyceraldehydes-3-phosphate dehydrogenase (GAPDH) transcripts. Primary calvarial osteoblasts from newborn wild-type mice were cultured as described in Materials and Methods. Bones from wild-type 12-week-old mice were prepared as described in Materials and Methods. Osteoclasts were purified from coculture bone marrow cells with calvarial osteoblasts. Rib cartilage from 4-week-old wild-type mice was dissected free of adherent soft tissues. Reverse transcription-PCRs performed in the absence of reverse transcriptase (−RT) failed to detect any transcripts (representative lane shown).

FIG. 3. Increased bone mineral density in *ChM-I*$^{-/-}$ mice (12 weeks of age). (A and B) Radiological analyses of femora. (A) Plain X-ray images of femora. (B) Bone mineral density of femora measured by dual-energy X-ray absorptiometry. Bars represent means ± standard errors for wild-type (black bars) and mutant (white bars) mice. **, $P < 0.01$ between the two groups. Statistical differences between groups were assessed by Student's *t* test. (C and D) Histological analyses of proximal tibiae. (C) Undecalcified plastic sections were stained with toluidine blue, which stains cartilage violet and bone clear. The panels on the right are higher magnifications of the boxed areas in the panels on the left. Bars, 0.5 mm (left) and 0.1 mm (right). (D) Undecalcified plastic sections were stained with TRAP, which stains mature chondroclasts (arrowheads) and osteoclasts (arrows) red. Bar, 0.1 mm. (E to K) Static bone histomorphometric analyses of trabecular bones in proximal tibiae from 12-week-old mice. (E) Percent bone volume per tissue volume (BV/TV) represents the ratio of bone volume to tissue volume and estimates bone mass. Percent osteoid surface per bone surface (OS/BS) (F) and osteoid thickness (O.Th) (G) represent the proportion and thickness of bone surface covered with unmineralized matrix, respectively. (H) Percent osteoblast surface per bone surface (Ob.S/BS) represents the proportion of bone surface covered with osteoblasts. Osteoclast number per bone perimeter (N.Oc/B.Pm) (I) and percent osteoclast surface per bone surface (Oc.S/BS) (J) estimate bone resorption as osteoclast number and surface, respectively, divided by bone surface. (K) Eroded surface represents the function of osteoclasts. ES/BS, eroded surface per bone surface. Bars represent means ± standard errors for wild-type (black bars) and mutant (white bars) mice. Asterisks indicate statistically significant differences between the two groups. *, **, and *** indicate *P* values of <0.05, <0.01, <0.005, respectively.

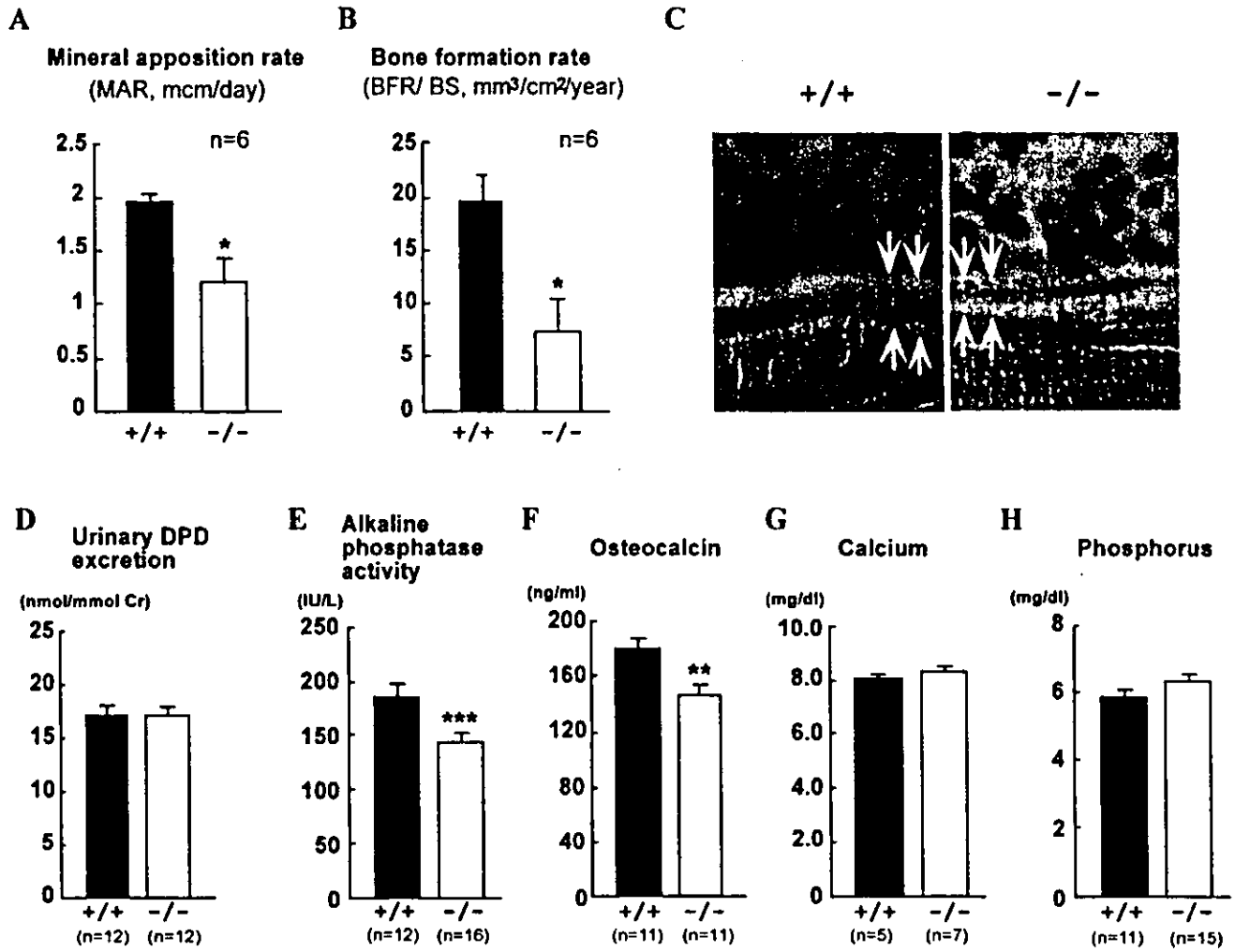

FIG. 5. Dynamic histomorphometric and serum biochemical parameters of bone metabolism in *ChM-I*$^{+/+}$ and *ChM-I*$^{-/-}$ mice (12 weeks of age). MAR (A) and BFR (B) are using sections from animals that were double-labeled with calcein in vivo. MAR and BFR measure the amount of bone that is mineralized or deposited per time unit and are based on the measurement of the distance between the two fluorescent labels. (C) Two calcein-labeled mineralization fronts of tibiae trabecular bones from *ChM-I*$^{+/+}$ and *ChM-I*$^{-/-}$ mice were visualized by fluorescent micrography. (D) Urinary deoxypyridinoline (DPD) excretion in 12-week-old wild-type and *ChM-I*$^{-/-}$ mice. (E) Alkaline phosphatase activity in serum. (F) Osteocalcin level in serum. (G) Calcium level in serum. (H) Phosphorus level in serum. Bars represent means ± standard errors for wild-type (black bars) and mutant (white bars) mice. Asterisks indicate statistically significant differences between the two groups (*, $P < 0.05$; **, $P < 0.01$, ***, $P < 0.005$).

DISCUSSION

ChM-I is a 25-kDa glycoprotein generated from a larger transmembrane precursor after posttranslational modification and proteolytic cleavage at a processing signal site (10). ChM-I was originally purified from bovine epiphyseal cartilage as a growth factor that stimulated anchorage-independent growth of chondrocytes in agarose (8) and induced proteoglycan synthesis (8). However, ChM-I also possesses inhibitory activity on the growth and tube morphogenesis of cultured vascular endothelial cells. Due to its bifunctional activities in vitro, it was thought that ChM-I might play a pivotal role in endochondral bone development during embryogenesis and in postnatal cartilage growth in vivo (27). However, our present observations with *ChM-I*$^{-/-}$ mice showed that ChM-I was not essential for normal cartilage formation and development. Indeed, our study revealed that ChM-I is more likely to be involved in normal bone remodeling, probably through regulating osteoclast and osteoblast numbers and functions. Detailed analysis of bones from *ChM-I*$^{-/-}$ mice showed that bone resorption was lower in comparison to bone formation, leading to increased bone mineral density and insufficient bone turnover.

Considering the marked cartilage phenotypes of mice deficient for angiogenic factors (6, 11, 33) or their inhibitors (7, 14), with which ChM-I was considered an equally potent factor in the cell culture systems (8, 9), the normal development of cartilage at embryonic and postnatal stages in *ChM-I*$^{-/-}$ mice was unexpected. Furthermore, no overt abnormalities were found in tests for rib fracture healing in adult *ChM-I*$^{-/-}$ mice (data not shown). It is possible that a functionally redundant factor may compensate for the lack of ChM-I activity in *ChM-*

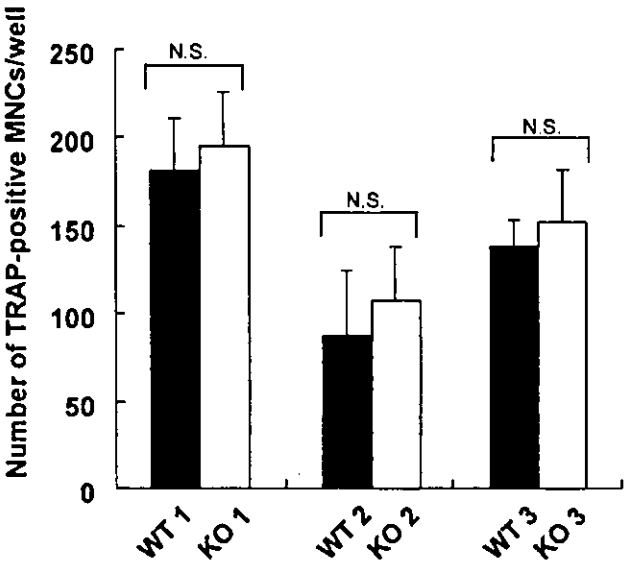

FIG. 6. In vitro osteoclastogenesis is not attached to ChM-I inactivation. Bone marrow macrophages were isolated from tibial bone marrow of 12-week-old mice and were induced to osteoclast formation by stimulation with 100 ng of M-CSF/ml and 100 ng of soluble rhRANKL/ml as described in Materials and Methods. TRAP-positive multinucleated cells (MNCs) per well were counted. Data are means ± standard deviations for four wells. WT, wild type; KO, knockout; N.S., not significant.

$I^{-/-}$ mice. While tenomodulin was once assumed to mimic ChM-I action in cartilage development, it was recently shown that its expression patterns do not overlap with that of ChM-I in cartilage (25). Moreover, tenomodulin expression was not affected by ChM-I inactivation in mice (data not shown). Thus, taken together, our study suggested the possible existence of a functionally redundant factor for ChM-I in chondrocytes.

As the only reported activity for ChM-I involved the stimulation of osteoblast proliferation and differentiation (19), which does not appear to explain the bone phenotype of the *ChM-I*$^{-/-}$ mice, the function of ChM-I in osteoclasts remains elusive. However, given the increased bone mineral density in *ChM-I*$^{-/-}$ mice, ChM-I expression in osteoblasts at low levels may regulate the expression of receptors or ligands that control the proliferation and/or differentiation of both osteoblasts and osteoclasts. In this respect, as decreased numbers of TRAP-positive mature osteoclasts were observed in *ChM-I*$^{-/-}$ mice, the possibility of the involvement of ChM-I in the RANKL-receptor activator of nuclear factor κB system of osteoclastogenesis (13, 15) is of interest and remains to be tested.

ACKNOWLEDGMENTS

We thank H. Murayama (Kureha Chemical Industry) for technical assistance with bone histology and Yasuhiro Kobayashi (Matsumoto Dental University) for helpful discussions about osteoclast generations. We thank R. Nakamura and H. Higuchi for manuscript preparation.

This work was supported by a grant-in-aid from the Japan Society for the Promotion of Science Research for the Future Program (to Y.H.) and priority areas from the Ministry of Education, Science, Sports and Culture of Japan (to S.K.).

REFERENCES

1. **Ducy, P., C. Desbois, B. Boyce, G. Pinero, B. Story, C. Dunstan, E. Smith, J. Bonadio, S. Goldstein, C. Gundberg, A. Bradley, and G. Karsenty.** 1996. Increased bone formation in osteocalcin-deficient mice. Nature **382**:448–452.
2. **Ducy, P., T. Schinke, and G. Karsenty.** 2000. The osteoblast: a sophisticated fibroblast under central surveillance. Science **289**:1501–1504.
3. **Gelb, D. E., R. N. Rosier, and J. E. Puzas.** 1990. The production of transforming growth factor-beta by chick growth plate chondrocytes in short term monolayer culture. Endocrinology **127**:1941–1947.
4. **Gerber, H. P., T. H. Vu, A. M. Ryan, J. Kowalski, Z. Werb, and N. Ferrara.** 1999. VEGF couples hypertrophic cartilage remodeling, ossification and angiogenesis during endochondral bone formation. Nat. Med. **5**:623–628.
5. **Gonzalez, A. M., M. Buscaglia, M. Ong, and A. Baird.** 1990. Distribution of basic fibroblast growth factor in the 18-day rat fetus: localization in the basement membranes of diverse tissues. J. Cell Biol. **110**:753–765.
6. **Haigh, J. J., H. P. Gerber, N. Ferrara, and E. F. Wagner.** 2000. Conditional inactivation of VEGF-A in areas of collagen2a1 expression results in embryonic lethality in the heterozygous state. Development **127**:1445–1453.
7. **Hankenson, K. D., S. D. Bain, T. R. Kyriakides, E. A. Smith, S. A. Goldstein, and P. Bornstein.** 2000. Increased marrow-derived osteoprogenitor cells and endosteal bone formation in mice lacking thrombospondin 2. J. Bone Miner. Res. **15**:851–862.
8. **Hiraki, Y., H. Inoue, K. Iyama, A. Kamizono, M. Ochiai, C. Shukunami, S. Iijima, F. Suzuki, and J. Kondo.** 1997. Identification of chondromodulin I as a novel endothelial cell growth inhibitor. Purification and its localization in the avascular zone of epiphyseal cartilage. J. Biol. Chem. **272**:32419–32426.
9. **Hiraki, Y., T. Kono, M. Sato, C. Shukunami, and J. Kondo.** 1997. Inhibition of DNA synthesis and tube morphogenesis of cultured vascular endothelial cells by chondromodulin-I. FEBS Lett. **415**:321–324.
10. **Hiraki, Y., H. Tanaka, H. Inoue, J. Kondo, A. Kamizono, and F. Suzuki.** 1991. Molecular cloning of a new class of cartilage-specific matrix, chondromodulin-I, which stimulates growth of cultured chondrocytes. Biochem. Biophys. Res. Commun. **175**:971–977.
11. **Holmbeck, K., P. Bianco, J. Caterina, S. Yamada, M. Kromer, S. A. Kuznetsov, M. Mankani, P. G. Robey, A. R. Poole, I. Pidoux, J. M. Ward, and H. Birkedal-Hansen.** 1999. MT1-MMP-deficient mice develop dwarfism, osteopenia, arthritis, and connective tissue disease due to inadequate collagen turnover. Cell **99**:81–92.
12. **Inoue, H., J. Kondo, T. Koike, C. Shukunami, and Y. Hiraki.** 1997. Identification of an autocrine chondrocyte colony-stimulating factor: chondromodulin-I stimulates the colony formation of growth plate chondrocytes in agarose culture. Biochem. Biophys. Res. Commun. **241**:395–400.
13. **Kong, Y. Y., H. Yoshida, I. Sarosi, H. L. Tan, E. Timms, C. Capparelli, S. Morony, A. J. Oliveira-dos-Santos, G. Van, A. Itie, W. Khoo, A. Wakeham, C. R. Dunstan, D. L. Lacey, T. W. Mak, W. J. Boyle, and J. M. Penninger.** 1999. OPGL is a key regulator of osteoclastogenesis, lymphocyte development and lymph-node organogenesis. Nature **397**:315–323.
14. **Kyriakides, T. R., Y. H. Zhu, L. T. Smith, S. D. Bain, Z. Yang, M. T. Lin, K. G. Danielson, R. V. Iozzo, M. LaMarca, C. E. McKinney, E. I. Ginns, and P. Bornstein.** 1998. Mice that lack thrombospondin 2 display connective tissue abnormalities that are associated with disordered collagen fibrillogenesis, an increased vascular density, and a bleeding diathesis. J. Cell Biol. **140**:419–430.
15. **Li, J., I. Sarosi, X. Q. Yan, S. Morony, C. Capparelli, H. L. Tan, S. McCabe, R. Elliott, S. Scully, G. Van, S. Kaufman, S. C. Juan, Y. Sun, J. Tarpley, L. Martin, K. Christensen, J. McCabe, P. Kostenuik, H. Hsu, F. Fletcher, C. R. Dunstan, D. L. Lacey, and W. J. Boyle.** 2000. RANK is the intrinsic hematopoietic cell surface receptor that controls osteoclastogenesis and regulation of bone mass and calcium metabolism. Proc. Natl. Acad. Sci. USA **97**:1566–1571.
16. **Li, X., N. Udagawa, K. Itoh, K. Suda, Y. Murase, T. Nishihara, T. Suda, and N. Takahashi.** 2002. p38 MAPK-mediated signals are required for inducing osteoclast differentiation but not for osteoclast function. Endocrinology **143**: 3105–3113.
17. **Malluche, H. H., D. Sherman, W. Meyer, and S. G. Massry.** 1982. A new semiautomatic method for quantitative static and dynamic bone histology. Calcif. Tissue Int. **34**:439–448.
18. **Marks, S. C., and D. C. Hermey.** 1996. The structure and development of bone, p. 3–14. *In* J. P. Bilezikian, L. G. Raise, and G. A. Rodan (ed.), Principles of bone biology. Academic Press, London, United Kingdom.
19. **Mori, Y., Y. Hiraki, C. Shukunami, S. Kakudo, M. Shiokawa, M. Kagoshima, H. Mano, Y. Hakeda, T. Kurokawa, F. Suzuki, and M. Kumegawa.** 1997. Stimulation of osteoblast proliferation by the cartilage-derived growth promoting factors chondromodulin-I and -II. FEBS Lett. **406**:310–314.
20. **Moses, M. A., J. Sudhalter, and R. Langer.** 1992. Isolation and characterization of an inhibitor of neovascularization from scapular chondrocytes. J. Cell Biol. **119**:475–482.
21. **Ogata, N., D. Chikazu, N. Kubota, Y. Terauchi, K. Tobe, Y. Azuma, T. Ohta, T. Kadowaki, K. Nakamura, and H. Kawaguchi.** 2000. Insulin receptor substrate-1 in osteoblast is indispensable for maintaining bone turnover. J. Clin. Investig. **105**:935–943.

22. **Parfitt, A. M., M. K. Drezner, F. H. Glorieux, J. A. Kanis, H. Malluche, P. J. Meunier, S. M. Ott, and R. R. Recker.** 1987. Bone histomorphometry: standardization of nomenclature, symbols, and units. Report of the ASBMR Histomorphometry Nomenclature Committee. J. Bone Miner. Res. 2:595–610.
23. **Sekine, K., H. Ohuchi, M. Fujiwara, M. Yamasaki, T. Yoshizawa, T. Sato, N. Yagishita, D. Matsui, Y. Koga, N. Itoh, and S. Kato.** 1999. Fgf10 is essential for limb and lung formation. Nat. Genet. 21:138–141.
24. **Shukunami, C., K. Iyama, H. Inoue, and Y. Hiraki.** 1999. Spatiotemporal pattern of the mouse chondromodulin-I gene expression and its regulatory role in vascular invasion into cartilage during endochondral bone formation. Int. J. Dev. Biol. 43:39–49.
25. **Shukunami, C., Y. Oshima, and Y. Hiraki.** 2001. Molecular cloning of tenomodulin, a novel chondromodulin-I related gene. Biochem. Biophys. Res. Commun. 280:1323–1327.
26. **Shukunami, C., S. Yamamoto, T. Tanabe, and Y. Hiraki.** 1999. Generation of multiple transcripts from the chicken chondromodulin-I gene and their expression during embryonic development. FEBS Lett. 456:165–170.
27. **Suzuki, F.** 1996. Roles of cartilage matrix proteins, chondromodulin-I and -II, in endochondral bone formation: a review. Connect. Tissue Res. 35:303–307.
28. **Takahashi, N., T. Akatsu, N. Udagawa, T. Sasaki, A. Yamaguchi, J. M. Moseley, T. J. Martin, and T. Suda.** 1988. Osteoblastic cells are involved in osteoclast formation. Endocrinology 123:2600–2602.
29. **Takeda, S., T. Yoshizawa, Y. Nagai, H. Yamato, S. Fukumoto, K. Sekine, S. Kato, T. Matsumoto, and T. Fujita.** 1999. Stimulation of osteoclast formation by 1,25-dihydroxyvitamin D requires its binding to vitamin D receptor (VDR) in osteoblastic cells: studies using VDR knockout mice. Endocrinology 140:1005–1008.
30. **Teitelbaum, S. L.** 2000. Bone resorption by osteoclasts. Science 289:1504–1508.
31. **Twal, W. O., R. Vasilatos-Younken, C. V. Gay, and R. M. Leach, Jr.** 1994. Isolation and localization of basic fibroblast growth factor-immunoreactive substance in the epiphyseal growth plate. J. Bone Miner. Res. 9:1737–1744.
32. **Uebelhart, D., E. Gineyts, M. C. Chapuy, and P. D. Delmas.** 1990. Urinary excretion of pyridinium crosslinks: a new marker of bone resorption in metabolic bone disease. Bone Miner. 8:87–96.
33. **Vu, T. H., J. M. Shipley, G. Bergers, J. E. Berger, J. A. Helms, D. Hanahan, S. D. Shapiro, R. M. Senior, and Z. Werb.** 1998. MMP-9/gelatinase B is a key regulator of growth plate angiogenesis and apoptosis of hypertrophic chondrocytes. Cell 93:411–422.
34. **Yagi, T., T. Tokunaga, Y. Furuta, S. Nada, M. Yoshida, T. Tsukada, Y. Saga, N. Takeda, Y. Ikawa, and S. Aizawa.** 1993. A novel ES cell line, TT2, with high germline-differentiating potency. Anal. Biochem. 214:70–76.
35. **Yagishita, N., Y. Yamamoto, T. Yoshizawa, K. Sekine, Y. Uematsu, H. Murayama, Y. Nagai, W. Krezel, P. Chambon, T. Matsumoto, and S. Kato.** 2001. Aberrant growth plate development in VDR/RXR gamma double null mutant mice. Endocrinology 142:5332–5341.
36. **Yoshizawa, T., Y. Handa, Y. Uematsu, S. Takeda, K. Sekine, Y. Yoshihara, T. Kawakami, K. Arioka, H. Sato, Y. Uchiyama, S. Masushige, A. Fukamizu, T. Matsumoto, and S. Kato.** 1997. Mice lacking the vitamin D receptor exhibit impaired bone formation, uterine hypoplasia and growth retardation after weaning. Nat. Genet. 16:391–396.

ELSEVIER

Bone 32 (2003) 341–349

BONE

www.elsevier.com/locate/bone

Involvement of vacuolar H^+-ATPase in incorporation of risedronate into osteoclasts

M. Takami,[a,1] K. Suda,[a,b,1] T. Sahara,[c] K. Itoh,[a] K. Nagai,[b,d] T. Sasaki,[c] N. Udagawa,[e] and N. Takahashi[f,*]

[a] *Department of Biochemistry, School of Dentistry, Showa University, Tokyo, Japan*
[b] *Department of Bioengineering, Tokyo Institute of Technology, Yokohama, Japan*
[c] *Department of Oral Histology, School of Dentistry, Showa University, Tokyo, Japan*
[d] *Department of Biological Chemistry, Chubu University, Kasugai, Japan*
[e] *Department of Biochemistry, Matsumoto Dental University, Shiojiri, Japan*
[f] *Institute for Oral Science, Matsumoto Dental University, Shiojiri, Japan*

Received 8 July 2002; revised 30 October 2002; accepted 24 November 2002

Abstract

Although osteoclasts incorporate bisphosphonates during bone resorption, the mechanism of this incorporation by osteoclasts is not known. We previously reported that bisphosphonates disrupt the actin rings (clear zones) formed in normal osteoclasts, but did not disrupt actin rings in osteoclasts derived from osteosclerotic oc/oc mice, which have a defect in the gene encoding vacuolar H^+-ATPase (V-ATPase). The present study showed that V-ATPase is directly involved in the incorporation of risedronate, a nitrogen containing bisphosphonate, into osteoclasts. Treatment of osteoclasts with risedronate disrupted actin rings and inhibited pit formation by osteoclasts on dentine slices. Bafilomycin A_1, a V-ATPase inhibitor, inhibited the pit-forming activity of osteoclasts but did not disrupt actin rings. Risedronate failed to disrupt actin rings in the presence of bafilomycin A_1. E-64, a lysosomal cysteine proteinase inhibitor, showed no inhibitory effect on the demineralization of dentine by osteoclasts but inhibited the digestion of dentine matrix proteins without disrupting actin rings. Risedronate disrupted actin rings even in the presence of E-64. Treatment of osteoclasts placed on plastic plates with risedronate also disrupted actin rings. Bafilomycin A_1 but not E64 prevented the disruption of actin rings in osteoclasts treated with risedronate on plastic plates. Inhibition of V-ATPase with bafilomycin A_1 also prevented disruption of actin rings by etidronate, a non-nitrogen-containing bisphosphonate. These results suggest that V-ATPase induced acidification beneath the ruffled borders of osteoclasts and subsequent bone demineralization triggers the incorporation of both nitrogen-containing and non-nitrogen-containing bisphosphonates into osteoclasts.

Keywords: Osteoclast; Bisphosphonate; Vacuolar H^+-ATPase; Acidification; Actin ring; Ruffled border

Introduction

Osteoclasts are highly polarized cells that form ruffled borders and clear zones to the bone surface during bone resorption [1–3]. Attachment of osteoclasts to extracellular proteins containing the RGD (Arg-Gly-Asp) sequence through vitronectin receptors is the first step in inducing the polarization of osteoclasts [4–6]. Polarized osteoclasts then secrete acid [7,8] and proteinases including cathepsins from the ruffled borders [9–11]. The secreted acids demineralize the bone matrix, and the proteinases digest bone matrix proteins including fibrous collagen. Finally, osteoclasts incorporate the digested bone matrices via endocytosis and release the matrix components from the apical membrane via exocytosis [12,13]. When osteoclasts are cultured on hard materials such as bone or dentine slices, they form ringed structures of F-actin dots called "actin rings," which exactly correspond to clear zones of bone-resorbing osteoclasts [14,15]. We have shown that disruption of actin

* Corresponding author. Institute for Oral Science, Matsumoto Dental University, 1780 Gobara, Hiro-oka, Shiojiri-shi, Nagano 399-0781, Japan.
E-mail address: takahashinao@po.mdu.ac.jp (N.Takahashi).
[1] Masamichi Takami and Koji Suda contributed equally to this study.

8756-3282/03/$ – see front matter © 2003 Elsevier Science (USA). All rights reserved.
doi:10.1016/S8756-3282(03)00024-3

rings by calcitonin and bisphosphonates results in inhibition of osteoclast function [16,17]. The actin ring, therefore, is thought to be a functional marker of activated osteoclasts [18,19].

Bisphosphonates are compounds with a carbon-substituted pyrophosphate structure (P-C-P) and are used for the clinical treatment of bone diseases such as osteoporosis, Paget's disease, and hypercalcemia associated with malignancy [20,21]. Biochemical and histological analyses have revealed the mechanism of the inhibitory effects of bisphosphonates on osteoclastic bone resorption as follows: When administered to animals or humans, bisphosphonates bind rapidly and tightly to bone mineral [21,22]. Osteoclasts incorporate bisphosphonates during bone resorption [17,20–22]. The incorporated bisphosphonates then induce the disruption of actin rings and apoptosis of osteoclasts [17,23,24]. Each step is critical for the inhibition of osteoclastic bone resorption by bisphosphonates.

We previously reported that tiludronate, a non-nitrogen-containing bisphosphonate, was specifically incorporated into polarized osteoclasts with ruffled borders and disrupted the actin rings [17]. Tiludronate failed to disrupt the actin rings of osteoclasts derived from osteosclerotic oc/oc mice, which have a defect in the gene encoding vacuolar H^+-ATPase (V-ATPase). However, tiludronate was able to completely disrupt the actin rings of osteoclasts derived from oc/oc mice as well as normal osteoclasts when given by microinjection into the cells [17]. These results suggest that oc/oc mouse-derived osteoclasts do not incorporate bisphosphonates and that V-ATPase is somehow involved in the incorporation of bisphosphonates.

V-ATPase is localized along the ruffled borders of osteoclasts and pumps protons out onto the bone surface [7,8,25]. Specific inhibitors of V-ATPase such as bafilomycin A_1 and concanamycin A inhibit the acidification of the bone surface below osteoclasts [25,26]. V-ATPase consists of two complexes, V_0 and V_1 [27,28]. The V_1 complex consists of subunits A, B, C, D, E, F, G, and H while the V_0 complex consists of at least three subunits, a, c, and d [28]. Subunit "a3 isoform" is strongly expressed in osteoclasts, and oc/oc mice have a 1.6-kbp deletion in the gene encoding this subunit [29]. Although the exact role of subunit a3 isoform is not known, it has been suggested that the a3 isoform is a component of the plasma membrane V-ATPase essential for bone resorption [30]. We have shown that V-ATPase in oc/oc mouse-derived osteoclasts is not localized to the ruffled borders but is evenly distributed throughout the cytoplasm [31]. On the basis of these results, we have hypothesized that the incorporation of bisphosphonates into polarized osteoclasts is regulated by the acidification of the extracellular microenvironment by V-ATPase.

In order to test this hypothesis, we examined the relationship between V-ATPase activity and the incorporation of bisphosphonates into osteoclasts using risedronate, a nitrogen-containing bisphosphonate. Treatment of osteoclasts with risedronate disrupted the actin rings and inhibited pit formation by osteoclasts on dentine slices and those o plastic plates. Inhibition of V-ATPase with bafilomycin A also inhibited the pit-forming activity of osteoclasts but di not disrupt the actin rings. Risedronate did not disrupt th actin rings of osteoclasts in the presence of bafilomycin A_1 These results suggest that acidification of the extracellula microenvironment by V-ATPase is essential for the incor poration of bisphosphonates into osteoclasts.

Materials and methods

Chemicals and dentine slices

Risedronate was supplied by Procter and Gamble Phar maceuticals (Cincinnati, OH). Bafilomycin A_1, concanamy cin A, E-64, etidronate, and 1,25-dihydroxyvitamin D $[1,25(OH)_2D_3]$ were obtained from Sigma Chemical Cc (St. Louis, MO). Dentine slices (4 mm in diameter, 0.2 mr in thickness) were made from an ivory block as describe previously [32]. Polyclonal antibodies against the 72-kD subunit of V-ATPase were kindly provided by Dr. Y Moriyama (Okayama University).

Animals and cell cultures

Five-week-old male and newborn ddY mice were ob tained from Sankyo Laboratories Animal Center (Tokyc Japan) and Saitama Experimental Animals (Saitama, Ja pan), respectively. Mice were killed by cervical dislocatio under light ether anesthesia. Primary osteoblasts were ob tained from calvariae of newborn mice by the conventiona method with collagenase and dispase as previously de scribed [32]. Bone marrow cells were obtained from tibia of adult male mice. Osteoclasts were generated in coculture of bone marrow cells (1×10^7 cells/dish) and primar osteoblasts (1×10^6 cells/dish) as described [32]. In brie cells were cultured in αMEM supplemented with 10% FC and 10nM $1,25(OH)_2D_3$ (20 ml/dish) in 100-mm tissu culture dishes (Corning, Inc., Corning, NY) at 37°C unde 5% CO_2 /95% air. Dishes were coated with type I collage gels (Nitta Gelatin, Osaka, Japan) just before the cells wer plated (5 ml/dish). Medium was replaced every 3 days wit fresh medium containing 10 nM $1,25(OH)_2D_3$. After 7 day in culture, osteoclasts generated on collagen gels were re covered by the digestion of the collagen gels with 0.1% collagenase solution. The recovered cells, which includ osteoclasts and osteoblasts, were used in the experiments

Actin staining

Osteoclasts recovered from cocultures were plated o dentine slices and cultured for 1 h in 96-well culture plate (1×10^5 cells/0.2 ml/well). Dentine slices were then care fully transferred into 48-well-culture plates, and then risedr onate (10 μM), etidronate (10 μM), calcitonin (10 ng/ml

bafilomycin A_1 (50 nM), and/or E-64 (100 nM) were added separately or in combination to the cultures. After a further 24 h, they were fixed with 3.7% formalin diluted with PBS and rinsed for 1 min with PBS containing 0.1% Triton X-100 (Sigma). F-actin in the cells was labeled with rhodamine-conjugated phalloidin (Molecular Probes, Eugene, OR) by incubating for 30 min in the dark [17]. After being washed with distilled water, actin rings were visualized under the microscope with ultraviolet light illumination. Osteoclasts recovered from cocultures were also placed in 48-well culture plates (1×10^5 cells/0.4 ml/well) and treated with risedronate (10 μM), etidronate (10 μM), calcitonin (10 ng/ml), bafilomycin A_1 (50 nM), and/or E-64 (100 nM). After culture for 24 h, they were fixed and subjected for F-actin staining. The number of actin rings on the dentine slices or plastic plates was counted. Bisphosphonates are rapidly adsorbed onto the dentine surface. The amount of risedronate or etidronate per dentine surface was 2 nmol/slice (12.6 mm^2). The results obtained from a typical experiment in three independent experiments were expressed as the means ± SD of four cultures. For statistical analysis of the results, groups were compared with Student's *t* test.

Analysis of pit-forming activity of osteoclasts

Osteoclasts recovered from the cocultures were placed on dentine slices (4 mm in diameter) in 96-well culture plates (1×10^5 cells/0.2 ml/well) and cultured for 1 h as described above. The dentine slices were then transferred into 48-well-culture plates (Corning) (0.4 ml/well) by the use of forceps. Risedronate (10 μM), calcitonin (10 ng/ml), bafilomycin A_1 (50 nM), and/or E-64 (100 nM) were added separately or in combination to the cultures. After the cells were cultured for another 24 h, the dentine slices were recovered and stained with Mayer's hematoxylin (Sigma) to visualize resorption pits. The number of resorption pits on the slices was counted using a microscope.

Analysis of V-ATPase distribution in osteoclasts by immunoelectron microscopic examination

Osteoclasts were cultured on dentine slices with or without bafilomycin A_1 (50 nM) for 24 h. Cultures were then fixed with a mixture of 4% formaldehyde and 0.1% glutaraldehyde in 0.1 M sodium cacodylate buffer (pH 7.3), demineralized in 10% EDTA, embedded in medium grade LR gold resin (London Resin Co. Ltd., Basingstoke, UK), and polymerized at -20°C under ultraviolet light. Ultrathin sections were mounted on Formver-coated nickel grids and treated with 10% BSA in PBS for 30 min to block the nonspecific binding of antiserum. The sections were incubated overnight at 4°C with rabbit anti-V-ATPase antibody and were then incubated for 1 h with goat anti-rabbit IgG conjugated with 10-nm colloidal gold particles (BioCell Research Laboratories, Cardiff, UK). After being rinsed with PBS and distilled water, the sections were stained with uranyl acetate and examined using a Hitachi H-7000 electron microscope.

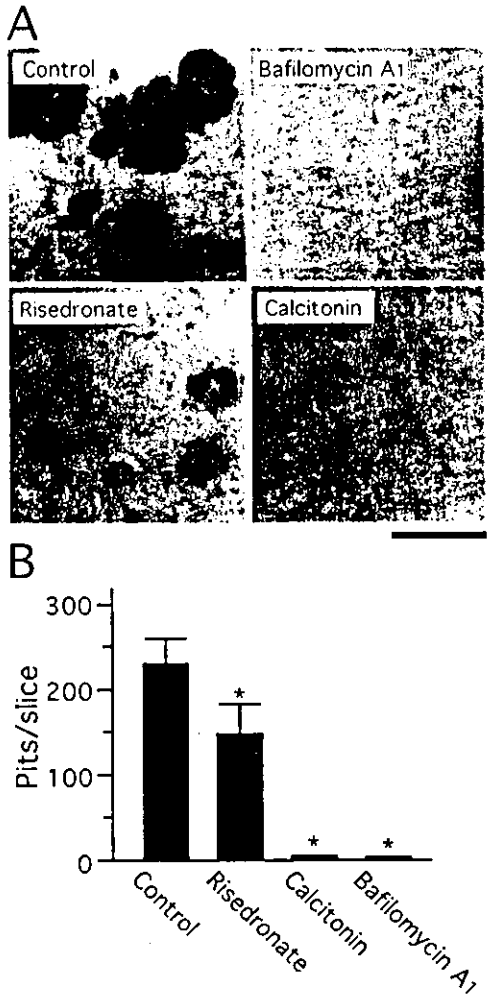

Fig. 1. Effects of risedronate, calcitonin, and bafilomycin A_1 on the pit-forming activity of osteoclasts. Osteoclasts were cultured on dentine slices in the absence or presence of risedronate (10 μM), bafilomycin A_1 (50 nM), and calcitonin (10 ng/ml). After cells were cultured for 24 h, they were removed from the dentine slices. Resorption pits on the slices were visualized by staining with Mayer's hematoxylin (A). The number of pits on the slices was counted (B). Data are expressed as means ± SD of four cultures. *Significantly different from the control culture: $P < 0.01$. Bar = 100 μm.

Results

Effects of risedronate, calcitonin, and bafilomycin A_1 on pit-forming activity and actin ring configuration of osteoclasts

When osteoclasts were cultured on dentine slices for 24 h, resorption pits were formed (Fig. 1A and B). Bafilomycin A_1, a potent inhibitor of V-ATPase, strongly inhib-

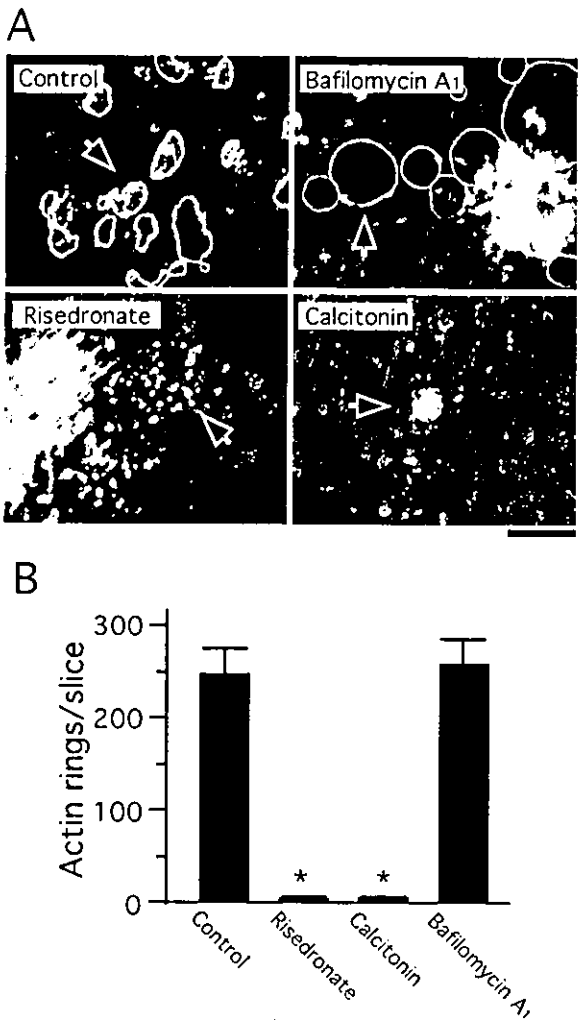

Fig. 2. Effects of risedronate, calcitonin, and bafilomycin A_1 on the actin ring configuration of osteoclasts. Osteoclasts were cultured on dentine slices for 24 h with or without risedronate (10 μM), bafilomycin A_1 (50 nM), or calcitonin (10 ng/ml). The cells were then fixed and labeled with rhodamine-conjugated phalloidin for visualization of F-actin (A). The number of actin rings on the slices was counted (B). Arrows indicate osteoclasts. Data are expressed as means ± SD of four cultures. *Significantly different from the control culture; $P < 0.01$. Bar = 100 μm.

ited the pit-forming activity of osteoclasts (Fig. 1A and B). Treatment of osteoclasts with risedronate reduced the number of pits by about 30% (Fig. 1B). The resorption pits formed in the presence of risedronate showed much less staining than those in the controls. This suggests that the depth of the pits formed in the presence of risedronate was less than that of controls. Calcitonin inhibited pit formation as potently as did bafilomycin A_1 (Fig. 1A and B).

In the control cultures, actin rings were observed in osteoclasts on dentine slices after culturing for 24 h (Fig. 2A and B). Treatment of the osteoclasts with risedronate or calcitonin for 24 h completely disrupted the actin rings. In contrast, treatment with bafilomycin A_1 did not disrupt the actin rings of osteoclasts even after 24 h. Concanamycin A (folimycin), another V-ATPase inhibitor, also inhibited the pit-forming activity of osteoclasts but did not disrupt the actin rings (data not shown). Interestingly, treatment with bafilomycin A_1 or with concanamycin A caused osteoclasts on dentine slices to expand (Fig. 2A). These results suggest that inhibition of the V-ATPase activity of osteoclasts suppresses the bone-resorbing activity but does not alter the configuration of actin rings in osteoclasts.

Effects of bafilomycin A_1 on risedronate and calcitonin disruption of actin ring configuration

To determine whether risedronate disruption of actin rings in osteoclasts requires V-ATPase activity, we treated osteoclasts with risedronate in the presence of bafilomycin A_1. Risedronate given alone caused disruption of the actin rings (Fig. 2A), but risedronate had no effect on actin rings in the presence of bafilomycin A_1 (Fig. 3A and B). In contrast, calcitonin disrupted actin rings even in the presence of bafilomycin A_1 (Fig. 3A and B). Treatment of osteoclasts with risedronate also did not disrupt actin rings in the presence of concanamycin A (data not shown). Nitrogen-containing bisphosphonates, including risedronate have been shown to inhibit osteoclast function by suppressing the mevalonate pathway: geranylgeranyl diphosphate or mevalonic acid prevented inhibition of osteoclasts by nitrogen-containing bisphosphonates but not by non-nitrogen-containing bisphosphonates [33–36]. Therefore, we examined the effects of etidronate, a non-nitrogen-containing bisphosphonate, on the actin ring configuration in osteoclasts placed on dentine slices (Fig. 3C). Etidronate disrupted actin rings in osteoclasts, and this effect was inhibited by bafilomycin A_1. These results suggest that V-ATPase activity is required for the incorporation of both nitrogen-containing and non-nitrogen-containing bisphosphonates into osteoclasts.

Effects of bafilomycin A_1 on V-ATPase localization in osteoclasts

We examined the subcellular localization of V-ATPase in osteoclasts treated with or without bafilomycin A_1 by immunoelectron microscopy. Immunogold particle distribution indicating V-ATPase was observed to be highly localized along the ruffled borders of dentine-resorbing osteoclasts (Fig. 4). In contrast, osteoclasts treated with bafilomycin A_1 did not form ruffled borders, and sparse V-ATPase localization was observed diffusely throughout the cytoplasm of osteoclasts (Fig. 4). These results suggest that disruption of V-ATPase localization to the ruffled border by bafilomycin A_1 results in the lack of acidification of the dentine surface.

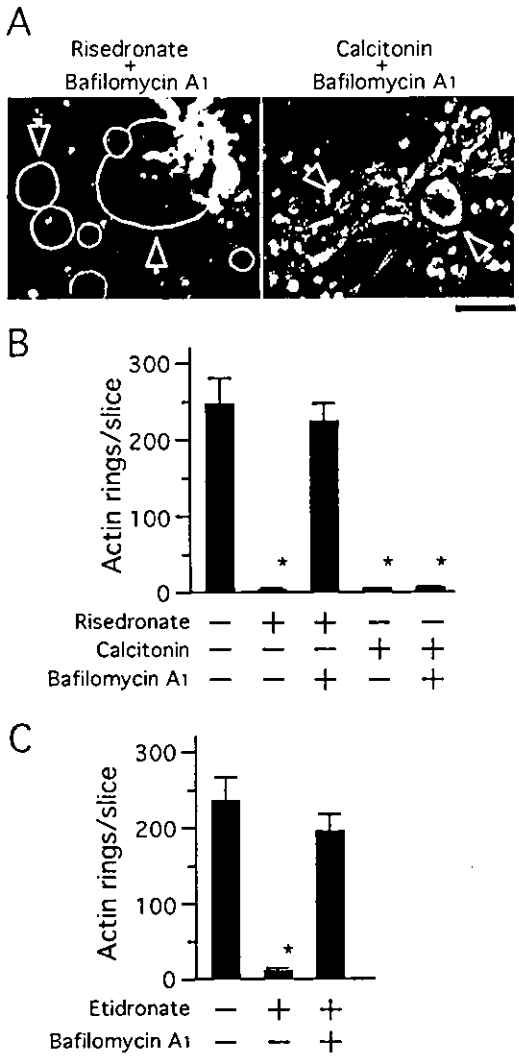

Fig. 3. Effects of bafilomycin A_1 on the disruption of actin rings induced by risedronate, etidoronate, and calcitonin. Osteoclasts were cultured on dentine slices for 24 h with or without risedronate (10 μM) or calcitonin (10 ng/ml) in the presence or absence of bafilomycin A_1 (50 nM) (A, B). Cells were then fixed and labeled with rhodamine-conjugated phalloidin for visualization of F-actin (A). Arrows indicate osteoclasts. The number of actin rings on the slices was counted (B). Osteoclasts were also cultured on dentine slices for 24 h with or without etidronate (10 μM) in the presence or absence of bafilomycin A_1 (50 nM) (C). Cells were then fixed and labeled with rhodamine-conjugated phalloidin, and the number of actin rings on the slices was counted. Data are expressed as means ± SD of four cultures. *Significantly different from the control culture; $P < 0.01$. Bar = 100 μm.

Effects of a proteinase inhibitor, E-64, on actin ring configuration of osteoclasts

Osteoclasts digest bone matrix proteins with proteinases after the matrix is demineralized with acid. We previously reported that when E-64, a lysosomal cysteine proteinase inhibitor, was added to the culture of osteoclasts on dentine slices, E-64 inhibited the digestion of dentine matrix proteins with proteinases but not demineralization of dentine with V-ATPase [37]. We then examined whether proteinase activity is required for risedronate-induced disruption of actin rings in osteoclasts. Osteoclasts were cultured for 24 h on dentine slices in the presence or absence of E-64, risedronate, or calcitonin (Fig. 5). E-64 did not disrupt the actin rings in osteoclasts (Fig. 5A). Risedronate and calcitonin disrupted the actin rings even in the presence of E-64 (Fig. 5A and B). These results suggest that risedronate can be incorporated into osteoclasts even when the digestion of bone matrix proteins is inhibited by E-64.

Effects of risedronate, calcitonin, bafilomycin A_1, and E64 on actin ring configuration of osteoclast placed on plastic plates

To prove whether the acidification is only important to release bisphosphonate from dentine slices, we examined the effects of risedronate on osteoclasts placed on plastic plates instead of dentine slices (Fig. 6). When osteoclasts on plastic plates were treated with risedronate, actin rings were disrupted as well as those on dentine slices (Fig. 6A and B). However, in the presence of bafilomycin A_1, risedronate failed to disrupt actin rings in osteoclasts on plastic plates. E64 did not affect risedronate-induced disruption of actin rings (Fig. 6A and B). These results suggest that V-ATPase activity is involved in incorporation of bisphosphonates by osteoclasts even in the absence of calcified dentine slices.

Discussion

Many lines of evidence indicate that V-ATPase and proteinases play essential roles in osteoclast-mediated bone resorption [7–11,29,38–40]. The present study showed that V-ATPase-induced acidification below the ruffled borders is important for incorporation of bisphosphonates into osteoclasts. Risedronate bound to dentine slices was able to disrupt actin rings in osteoclasts. This effect was blocked by inhibition of V-ATPase with bafilomycin A_1 but not by inhibition of proteinases with E-64. These results suggest that V-ATPase-mediated but not proteinase-mediated degradation of dentine matrix proteins is involved in the incorporation of bisphosphonates into osteoclasts.

Nitrogen-containing bisphosphonates such as pamidronate, alendronate, and risedronate inhibit the mevalonate pathway in osteoclasts [33–36]. Non-nitrogen-containing bisphosphonates such as etidronate do not inhibit the mevalonate pathway and thus inhibit osteoclasts via a different mechanism [33–36]. In agreement with these findings, either geranylgeranyl diphosphate or mevalonic acid added to the osteoclast cultures prevented the disruption of actin rings induced by risedronate, but not that induced by etidronate (data not shown). These results suggest that both nitrogen-containing and non-nitrogen-containing bisphosphonates are incorporated into osteoclasts in the same man-

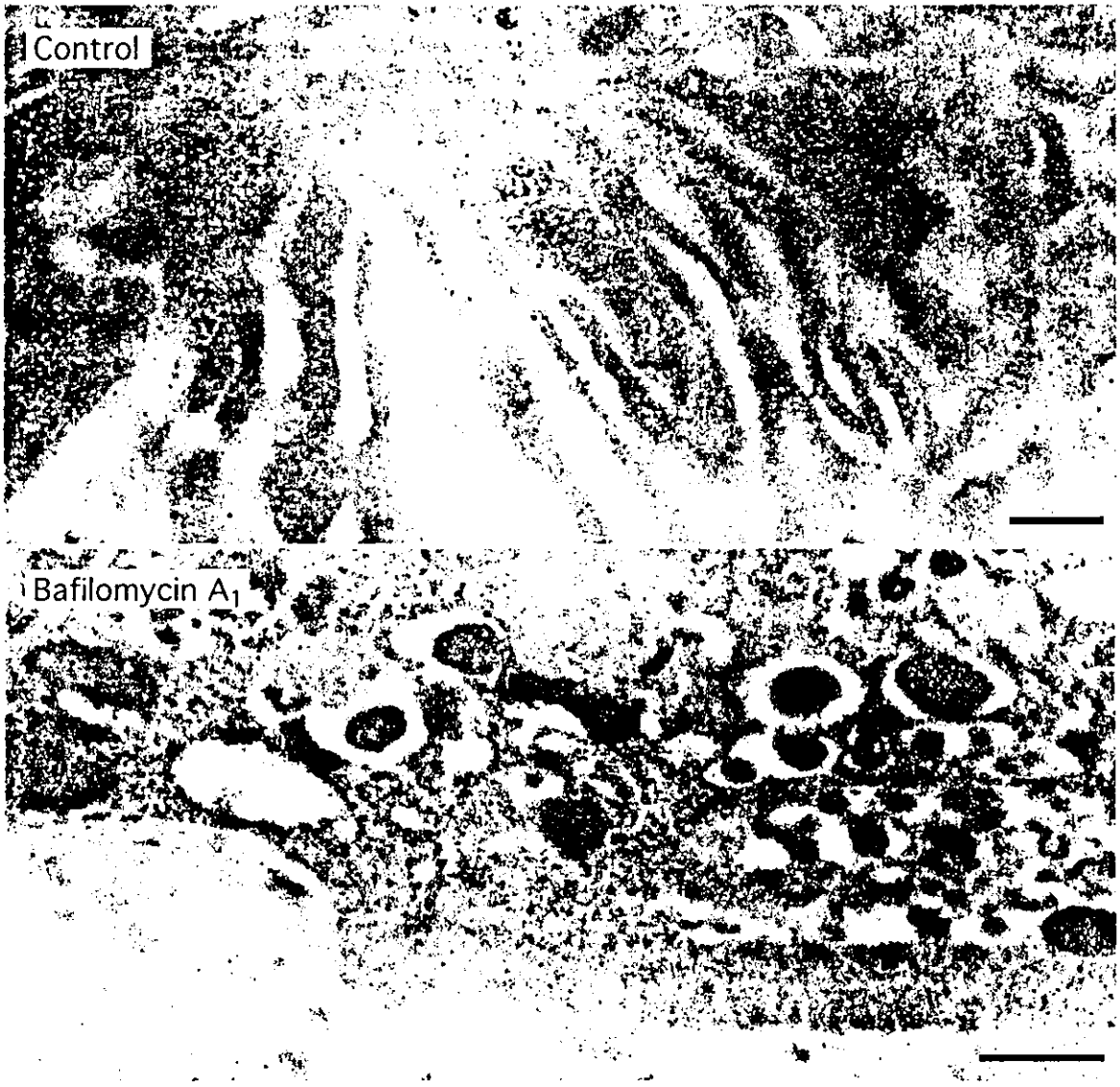

Fig. 4. Distribution of immunogold particles indicating V-ATPase in the osteoclasts treated with and without bafilomycin A_1. Osteoclasts were cultured dentine slices for 24 h in the absence or presence of bafilomycin A_1 (50 nM). Ultrathin sections of osteoclasts were prepared and incubated with rab anti-V-ATPase antibodies and then with goat anti-rabbit IgG conjugated with 10-nm colloidal gold particles. Immunogold particles, which indicate t distribution of V-ATPase, appear as black dots in photomicrographs. Bar = 500 nm.

ner, but the intracellular actions of the two types of bisphosphonates are different.

Ito et al. [41] reported that osteoclasts in oc/oc mice could incorporate bisphosphonates administered in vivo. Apoptosis of osteoclasts in oc/oc mice was observed after 3 days of a single injection of 1 mg/kg of incadronate. Since osteoclasts of oc/oc mice fail to form ruffled borders, it is suggested that osteoclasts incorporate bisphosphonate from a site different from ruffled borders. Halasy-Nagy et al. [42] showed that relatively high concentrations of alendronate or risedronate also induce apoptosis of osteoclasts. In our experiments, risedronate at the concentrations used induced apoptosis of a small number of osteoclasts (less than 10%). These results suggest that the disruption of actin rings may not necessarily result in apoptosis of osteoclasts and that bisphosphonates at high concentrations may enter into c teoclasts and induce apoptosis of osteoclasts.

Immunoelectron microscopic analysis showed that ' ATPase was highly localized to the ruffled border in norn polarized osteoclasts, but that it was diffusely distribut throughout the cytoplasm in osteoclasts treated with bafil mycin A_1. Lee et al. [43] found that V-ATPase direc binds to the microfilaments during the process of osteocl activation. They also suggested that the B subunit of ATPase contains a filamentous actin binding site [44]. I terestingly, bafilomycin A_1 induced the expansion of os oclasts. These data, together with our findings, suggest tl bafilomycin A_1 may inhibit the interaction between micr filaments and V-ATPase and that this interaction is requir for V-ATPase enzymatic activity.

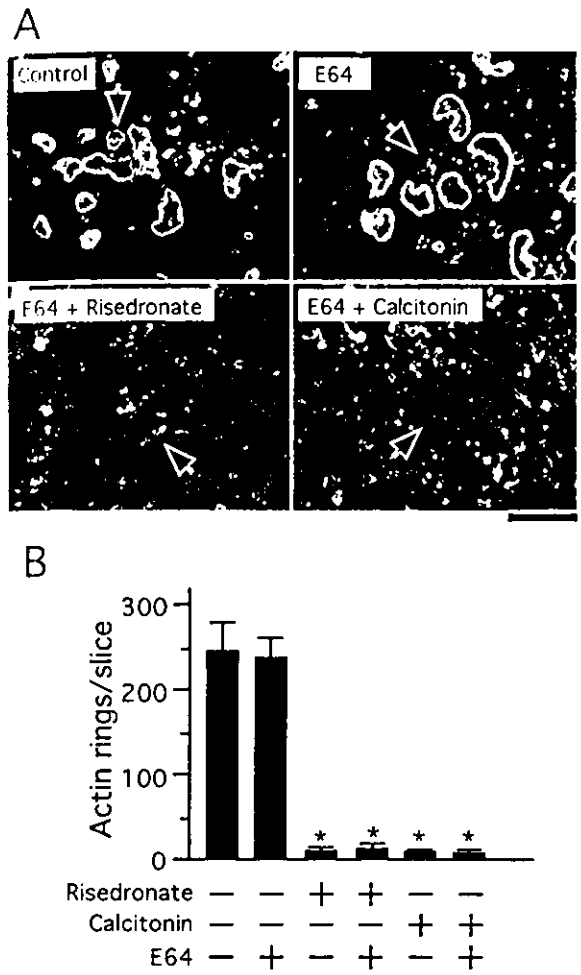

Fig. 5. Effects of E-64 on the disruption of actin rings induced by risedronate and calcitonin. Osteoclasts were cultured on dentine slices for 24 h with or without risedronate (10 μM) or calcitonin (10 ng/ml) in the presence or absence of E-64 (100 nM). Cells were fixed and labeled with rhodamine-conjugated phalloidin for visualization of F-actin (A). The number of actin rings on the slices was counted (B). Arrows indicate osteoclasts. Data are expressed as means ± SD of four cultures. *Significantly different from the control culture; $P < 0.01$. Bar = 100 μm.

We previously reported that tiludronate failed to inhibit the process of actin ring formation by osteoclasts on dentine slices, but disrupted actin rings soon after osteoclasts began to form resorption pits [17]. Actin rings of oc/oc mouse-derived osteoclasts showed strong resistance to tiludronate added to the culture medium, but the microinjection of tiludronate into oc/oc mouse-derived osteoclasts as well as into normal osteoclasts disrupted actin rings within 20 min [17]. In the present study, resorption pits slightly stained with dye were observed on the surface of dentine slices even in the presence of risedronate. These results supports the notion that bone resorption is a critical process for incorporation of bisphosphonates into osteoclasts.

Okahashi et al. [45] reported that inhibition of V-ATPase by bafilomycin A_1 or concanamycin A suppressed the survival of TRAP-positive osteoclasts due to inducing apoptosis. We noticed that TRAP activity was markedly reduced in osteoclasts by the treatment with bafilomycin A_1 and concanamycin A (data not shown). TRAP-positive cells were hardly detected in the cultures of osteoclasts treated with V-ATPase inhibitors. However, F-actin staining showed that the number of multinucleated cells with actin rings was not significantly reduced in the culture treated with V-ATPase inhibitors at the concentrations used. Actin rings of TRAP-negative multinucleated cells were completely disrupted by calcitonin, suggesting that TRAP-negative multinucleated cells induced by V-ATPase inhibitors possess one of the most important characteristics of osteoclasts, the responsiveness to calcitonin. Further studies will elucidate the relationship between enzyme activities of V-ATPase and TRAP in osteoclasts.

We previously reported that osteoclasts polarize not only on dentine slices but also on plastic plates [15]. Osteoclasts

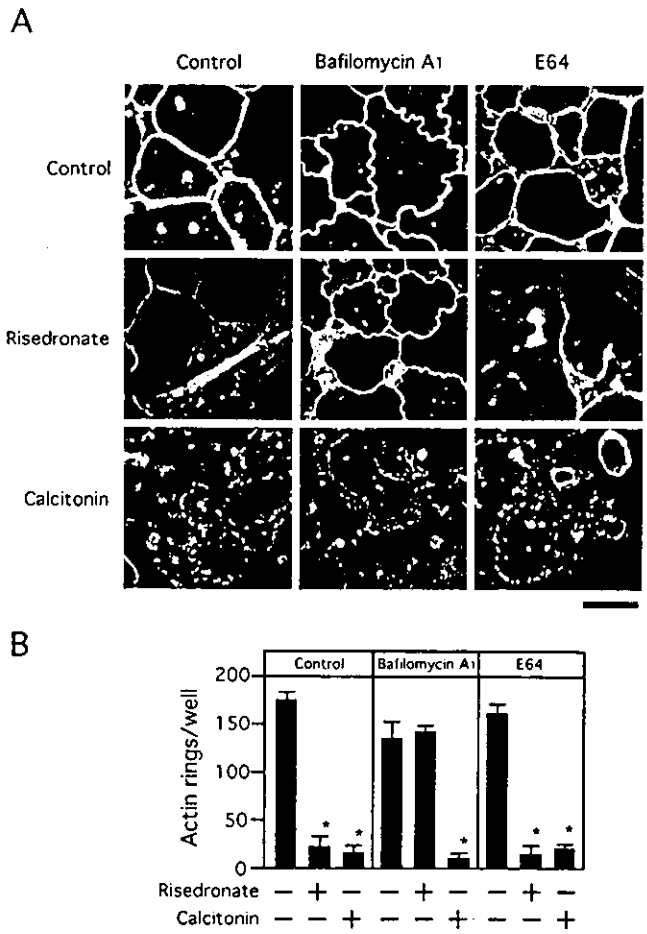

Fig. 6. Effects of risedronate, calcitonin, bafilomycin A_1, and E64 on actin ring configuration in osteoclasts placed on plastic plates. Osteoclasts were cultured in 48-well culture plates in the presence or absence of risedronate (10 μM) or calcitonin (10 ng/ml) in combination with bafilomycin A_1 (50 nM) or E-64 (100 nM). After cells were cultured for 24 h, cells were fixed and labeled with rhodamine-conjugated phalloidin for visualization of F-actin (A). The number of actin rings in the wells was counted (B). Data are expressed as means ± SD of four cultures. *Significantly different from the control culture; $P < 0.01$. Bar = 100 μm.

placed on plastic plates formed actin rings, and V-ATPase was localized along the apical membrane in a much higher density than along the basolateral membrane. Silver et al. [46] showed that osteoclasts generate an acidic mocroenvironment (pH 3.0 or less) specifically in the attachment zone between the cell and the base of culture dish using pH microelectrodes. These findings support our notion that acidification of microenvironment by V-ATPase activity is important for the uptake of bisphosphonate even in the absence of calcified matrix.

The final question in this study addresses why V-ATPase activity is important for the uptake of bisphosphonates by osteoclasts. Although the precise mechanism of the specific incorporation of bisphosphonates by bone-resorbing osteoclasts is still unknown, our study may provide some possible answers to this question as follows: (1) Bisphosphonates have the "P-C-P" backbone structure with various side chains on the carbon [20,21]. Acidic conditions below the ruffled borders of osteoclasts increase the amount of nonpolar types of bisphosphonates, which may easily pass through the plasma membranes of osteoclasts. We determined the dissociation constants of risedronate in H_2O and found that risedronate possesses five pK_a values, 1.6, 2.2, 5.9, 7.1, and 11.7 (data not shown). This indicates that the polarity of risedronate changes significantly depending on the acidity of the microenvironment. A decrease in the polarity of bisphosphonates due to acidic conditions may increase their accessibility to the plasma membranes of cells. (2) Since the refractoriness to bisphosphonates was observed with lack of ruffled borders, it is possible that the formation of ruffled borders accompanied by acidification is important for the incorporation of bisphosphonates. Furthermore, if osteoclasts express proteins essential to specific incorporation of bisphosphonates, the proteins will function at the ruffled borders. (3) Inhibition of V-ATPase in osteoclasts may stabilize the structure of actin rings to resist bisphosphonates. Further studies are necessary to elucidate the precise mechanism of specific incorporation of bisphosphonates by polarized osteoclasts.

In conclusion, V-ATPase acidification of the extracellular microenvironment under the ruffled border of osteoclasts appears to be essential for the incorporation of bisphosphonates into osteoclasts. This observation may help optimize the design of new drugs for incorporation by osteoclasts.

Acknowledgments

This study was supported in part by grants-in-aid (13557155 and 13470394), the High-Technology Research Center Project from the Ministry of Education, Culture, Sports, Science, and Technology of Japan, and a grant from Aventis Pharma Ltd., Takeda Chemical Industries, Ltd., and Ajinomoto Co., Inc.

References

[1] Chambers TJ. Regulation of the differentiation and function of o oclasts. J Pathol 2000;192:4–13.
[2] Teitelbaum SL. Bone resorption by osteoclasts. Science 2000;2 1504–8.
[3] Roodman GD. Cell biology of the osteoclast. Exp Hematol 1999 1229–41.
[4] Lakkakorpi PT, Horton MA, Helfrich MH, Karhukorpi Väänänen HK. Vitronectin receptor has a role in bone resorption does not mediate tight sealing zone attachment of osteoclasts to bone surface. J Cell Biol 1991;115:1179–86.
[5] Duong LT, Lakkakorpi P, Nakamura I, Rodan GA. Integrins signaling in osteoclast function. Matrix Biol 2000;19:97–105.
[6] Nakamura I, Pilkington MF, Lakkakorpi PT, Lipfert L, Sims : Dixon SJ, Rodan GA, Duong LT. Role of $\alpha_v\beta_3$ integrin in osteo migration and formation of the sealing zone. J Cell Sci 1999; 3985–93.
[7] Blair HC, Teitelbaum SL, Ghiselli R, Gluck S. Osteoclastic b resorption by a polarized vacuolar proton pump. Science 1989; 855–7.
[8] Väänänen HK, Karhukorpi EK, Sundquist K, Wallmark B, Roin I, Hentunen T, Tuukkanen J, Lakkakorpi P. Evidence for the pres of a proton pump of the vacuolar H^+-ATPase type in the ru borders of osteoclasts. J Cell Biol 1990;111:1305–11.
[9] Tezuka K, Nemoto K, Tezuka Y, Sato T, Ikeda Y, Kobori M, Eg H H, Hakeda Y, Kumegawa M. Identification of matrix metallo teinase 9 in rabbit osteoclasts. J Biol Chem 1994;269:15006–9.
[10] Dodds RA, Connor JR, Drake FH, Gowen M. Expression of cathe K messenger RNA in giant cells and their precursors in hu osteoarthritic synovial tissues. Arthritis Rheum 1999;42:1588–9
[11] Sasaki T, Ueno-Matsuda E. Cysteine-proteinase localization in oclasts: an immunocytochemical study. Cell Tissue Res 1993; 177–9.
[12] Nesbitt SA, Horton MA. Trafficking of matrix collagens thr bone-resorbing osteoclasts. Science 1997;276:266–9.
[13] Salo J, Lehenkari P, Mulari M, Metsikko K, Väänänen HK. Ren of osteoclast bone resorption products by transcytosis. Science 1 276:270–3.
[14] Väänänen HK, Horton M. The osteoclast clear zone is a specia cell–extracellular matrix adhesion structure. J Cell Sci 1995 2729–32.
[15] Nakamura I, Takahashi N, Sasaki T, Jimi E, Kurokawa T, Su Chemical and physical properties of the extracellular matri required for the actin ring formation in osteoclasts. J Bone Mine 1996;11:1873–9.
[16] Suzuki H, Nakamura I, Takahashi N, Ikuhara T, Matsuzaki K, I Y, Hori M, Suda T. Calcitonin-induced changes in the cytoske are mediated by a signal pathway associated with protein kinase osteoclasts. Endocrinology 1996;137:4685–90.
[17] Murakami H, Takahashi N, Sasaki T, Udagawa N, Tanaka S, I mura I, Zhang D, Barbier A, Suda T. A possible mechanism f specific action of bisphosphonates on osteoclasts: tiludronate p entially affects polarized osteoclasts having ruffled borders. 1995;17:137–44.
[18] Suda T, Nakamura I, Jimi E, Takahashi N. Regulation of oste function. J Bone Miner Res 1997;12:869–79.
[19] Burgess TL, Qian Y, Kaufman S, Ring BD, Van G, Capparo Kelley M, Hsu H, Boyle WJ, Dunstan CR, Hu S, Lacey DL ligand for osteoprotegerin (OPGL) directly activates mature oclasts. J Cell Biol 1999;145:527–38.
[20] Fleisch H. Bisphosphonates: mechanisms of action. Endoc 1998;19:80–100.
[21] Russell RG, Rogers MJ. Bisphosphonates: from the laboratory clinic and back again. Bone 1999;25:97–106.

[22] Sato M, Grasser W, Endo N, Akins R, Simmons H, Thompson DD, Golub E, Rodan GA. Bisphosphonate action. Alendronate localization in rat bone and effects on osteoclast ultrastructure. J Clin Invest 1991;88:2095–105.
[23] Watanabe J, Amizuka N, Noda T, Ozawa H. Cytochemical and ultrastructural examination of apoptotic odontoclasts induced by bisphosphonate administration. Cell Tissue Res 2000;301:375–87.
[24] Hughes DE, Wright KR, Uy HL, Sasaki A, Yoneda T, Roodman GD, Mundy GR, Boyce BF. Bisphosphonates promote apoptosis in murine osteoclasts in vitro and in vivo. J Bone Miner Res 1995;10:1478–87.
[25] Sasaki T, Hong MH, Udagawa N, Moriyama Y. Expression of vacuolar H^+-ATPase in osteoclasts and its role in resorption. Cell Tissue Res 1994;278:265–71.
[26] Inoue M, Yoshida H, Akisaka T. Visualization of acidic compartments in cultured osteoclasts by use of an acidotrophic amine as a marker for low pH. Cell Tissue Res 1999;298:527–37.
[27] Wieczorek H, Grber G, Harvey WR, Huss M, Merzendorfer H, Zeiske W. Structure and regulation of insect plasma membrane H^+-ATPase. J Exp Biol 2000;203:127–35.
[28] Futai M, Oka T, Sun-Wada G, Moriyama Y, Kanazawa H, Wada Y. Luminal acidification of diverse organelles by V-ATPase in animal cells. J Exp Biol 2000;203:107–16.
[29] Scimeca JC, Franchi A, Trojani C, Parrinello H, Grosgeorge J, Robert C, Jaillon O, Poirier C, Gaudray P, Carle GF. The gene encoding the mouse homologue of the human osteoclast-specific 116-kDa V-ATPase subunit bears a deletion in osteosclerotic (oc/oc) mutants. Bone 2000;26:207–13.
[30] Toyomura T, Oka T, Yamaguchi C, Wada Y, Futai M. Three subunit a isoforms of mouse vacuolar H^+-ATPase. Preferential expression of the a3 isoform during osteoclast differentiation. J Biol Chem 2000; 275:8760–65.
[31] Nakamura I, Takahashi N, Udagawa N, Moriyama Y, Kurokawa T, Jimi E, Sasaki T, Suda T. Lack of vacuolar proton ATPase association with the cytoskeleton in osteoclasts of osteosclerotic (oc/oc) mice. FEBS Lett 1997;401:207–12.
[32] Suda T, Jimi E, Nakamura I, Takahashi N. Role of 1α, 25-dihydroxyvitamin D_3 in osteoclast differentiation and function. Methods Enzymol 1997;282:223–35.
[33] Luckman SP, Hughes DE, Coxon FP, Graham R, Russell G, Rogers MJ. Nitrogen-containing bisphosphonates inhibit the mevalonate pathway and prevent post-translational prenylation of GTP-binding proteins, including Ras. J Bone Miner Res 1998;13:581–9.
[34] Fisher JE, Rogers MJ, Halasy JM, Luckman SP, Hughes DE, Masarachia PJ, Wesolowski G, Russell RG, Rodan GA, Reszka AA. Alendronate mechanism of action: geranylgeraniol, an intermediate in the mevalonate pathway, prevents inhibition of osteoclast formation, bone resorption, and kinase activation in vitro. Proc Natl Acad Sci USA 1999;96:133–8.
[35] Fisher JE, Rodan GA, Reszka AA. In vivo effects of bisphosphonates on the osteoclast mevalonate pathway. Endocrinology 2000;141:4793–6.
[36] Coxon FP, Helfrich MH, Van't Hof R, Sebti S, Ralston SH, Hamilton A, Rogers MJ. Protein geranylgeranylation is required for osteoclast formation, function, and survival: inhibition by bisphosphonates and GGTI-298. J Bone Miner Res 2000;15:1467–76.
[37] Sasaki T. Recent advances in the ultrastructural assessment of osteoclastic resorptive functions. Microsc Res Tech 1996;33:182–91.
[38] Li YP, Chen W, Liang Y, Li E, Stashenko P. Atp6i-deficient mice exhibit severe osteopetrosis due to loss of osteoclast-mediated extracellular acidification. Nat Genet 1999;23:447–51.
[39] Kornak U, Schulz A, Friedrich W, Uhlhaas S, Kremens B, Voit T, Hasan C, Bode U, Jentsch TJ, Kubisch C. Mutations in the a3 subunit of the vacuolar H^+-ATPase cause infantile malignant osteopetrosis. Hum Mol Genet 2000;9:2059–63.
[40] Michigami T, Kageyama T, Satomura K, Shima M, Yamaoka K, Nakayama M, Ozono K. Novel mutations in the a3 subunit of vacuolar H^+-adenosine triphosphatase in a Japanese patient with infantile malignant osteopetrosis. Bone 2002;30:436–9.
[41] Ito M, Amizuka N, Nakajima T, Ozawa H. Bisphosphonate acts on osteoclasts independent of ruffled borders in osteosclerotic (oc/oc) mice. Bone 2001;28:609–16.
[42] Halasy-Nagy JM, Rodan GA, Reszka AA. Inhibition of bone resorption by alendronate and risedronate does not require osteoclast apoptosis. Bone 2001;29:553–9.
[43] Lee BS, Gluck SL, Holliday LS. Interaction between vacuolar H^+-ATPase and microfilaments during osteoclast activation. J Biol Chem 1999;274:29164–71.
[44] Holliday LS, Lu M, Lee BS, Nelson RD, Solivan S, Zhang L, Gluck SL. The amino-terminal domain of the B subunit of vacuolar H^+-ATPase contains a filamentous actin binding site. J Biol Chem 2000; 275:32331–7.
[45] Okahashi N, Nakamura I, Jimi E, Koide M, Suda T, Nishihara T. Specific inhibitors of vacuolar H^+-ATPase trigger apoptotic cell death of osteoclasts. J Bone Miner Res 1997;12:1116–23.
[46] Silver IA, Murrills RJ, Etherington DJI. Microelectrode studies on the acid microenvironment beneath adherent macrophages and osteoclasts. Exp Cell Res 1988;175:266–76.